UNIVERSITY OF COPENHAGEN

A thesis presented to the Faculty of Science in partial fulfillment of the requirements for the degree

Master of Science in Medical Physics

Image Guided & Adaptive Radiotherapy in Esophageal Cancer

Kassiani Tsemperlidi

kassiani.tsemperlidi@regionh.dk

Supervisors: Jens Jørgen Gaardhøje, Mirjana Josipovic

October 30, 2020

ACKNOWLEDGEMENTS

First and foremost, I would like to thank my supervisors **Jens Jørgen Gaardhøje** and **Mirjana Josipovic** for giving me the opportunity to work on this project and expand my skills. **Mirjana**, thank you for believing in me and give me the chance to gain significant knowledge and be part of the medical physics research. I feel lucky for collaborating with you, despite your busy clinical work you always found time when I needed and your critical sense and observations were only beneficial for me. **Jens**, I greatly appreciate your trust in me for being my internal supervisor, without your consent this project would not exist.

A big thank you I owe to **Ivan Richter Vogelius** and **Katrin Håkansson** for your precious time despite your busy schedule. Both gave me great guidance and inspiration during the second and critical part of my project. I am grateful for working within your research group and participate to research group meetings, it had benefited me in many ways. I appreciate very much the help of my colleague **Emmanouil Terzidis** for sharing his skills and helping me when I needed.

Finally, I would like to thank my boyfriend **Nikos** and my parents- **Dimitris** & **Antonia**- for believing in me and supporting me during the stressful moments.

ABBREVIATIONS LIST

- SD : Standard Deviation
- LA : Lateral
- PA : Posterior-Anterior
- SI : Superior-Inferior
- CT : Computed tomography
- CBCT : Cone-beam computed tomography
- RIR : Rigid image registration
- DIR : Deformable image registration
- DVH : Dose-volume histogram
- GTV : Gross tumor volume
- CTV : Clinical target volume
- PTV : Planning target volume

ABSTRACT

The purpose of this study is to examine the current clinical workflow in radiotherapy in oesophageal cancer and suggest new approaches if needed. The thesis is divided into two parts, in the first one we compared different image registration strategies for image-guided radiotherapy, whereas in the second we investigated the efficiency and coverage of the dose planning through the whole treatment period. We included 20 consecutive patients, treated for oesophageal cancer at Rigshospitalet in 2017, with 50 Gy in 25 fractions. All patients have been scanned daily with cone-beam CT (CBCT) for image guidance, resulting in 25 CBCT scans per patient.

For the first part of the study, we re-registered 6 CBCTs per patient (nr 1, 5, 10, . . . 25) with focus on three different structures: bones (primarily the spine), gross tumor volume (GTVp), and clinical target volume (CTV). The image registrations were performed rigidly in the Aria platform, Image Registration (by Varian Medical Systems inc.). We compared the differences between different registration strategies and evaluated systematic and random uncertainties according to van Herk et al. (IJROBP 2000) and calculated the margin sizes in each case.

During the second part, due to the time limitation, we studied 3 out of 25 patients. For each of them, we performed a deformable registration between the planning CT and the CBCT scans in order to evaluate the coverage of the original dose plan on the observed anatomy changes. The image deformations were performed in the Velocity platform by Varian Medical Systems inc. We compared the dose-volume histograms focusing on CTV coverage.

Results: We found that all three RIR strategies had lower systematic than random uncertainties. Our PTV margin values for bone match under the assumption of ”perfect soft tissue

match" were larger than the clinical limits (7mm) however as we have shown our hypothesis on "perfect soft tissue match" did not hold.

CONTENTS

LIST OF FIGURES

LIST OF TABLES

Part I

BACKGROUND

1

BACKGROUND & THEORY

1.1 ESOPHAGUS CANCER

Cancer is a disease caused by an uncontrolled division of abnormal cells in a part or parts of the body. In this project, we are studying esophageal cancer which is the cancer of the esophagus. Esophagus is the body part that connects the throat to the stomach and lies between the trachea and spine. It is a hollow muscular tube with several layers. As it is mentioned in [14], cancer initiates from the inner layer, called mucosa, and grows outwards (see fig. 1).

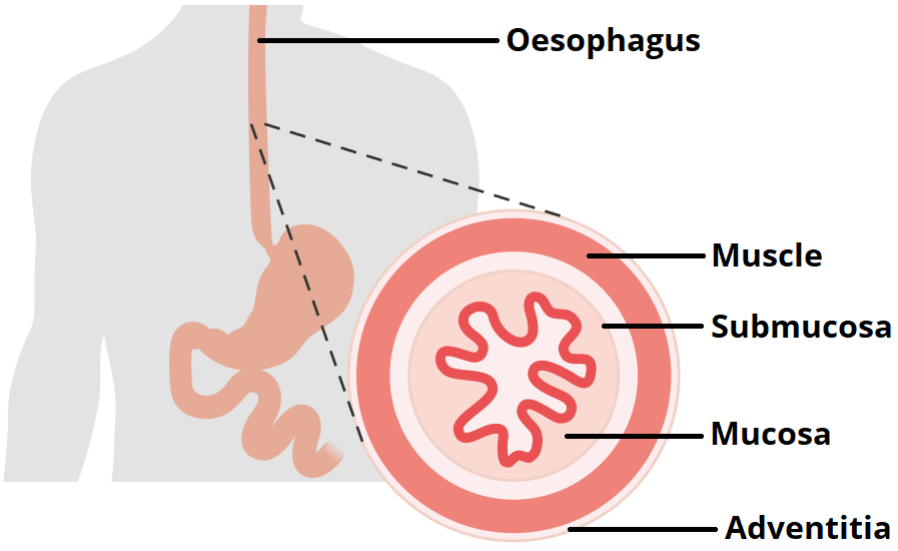

Figure 1: Esophagus layers (from Cancer Research UK [14])

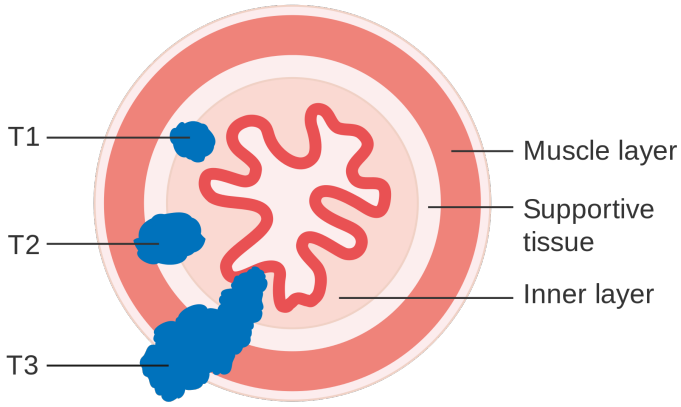

Figure 2: Cancer growth inside esophagus (from Cancer Research UK [14])

There are two main types of esophageal cancer: squamous cell carcinoma and adenocarcinoma. Squamous cell carcinoma arises from the epithelial cells that line the esophagus and are usually located behind the chest cavity around the neck region. Adenocarcinoma arises from glandular cells present in the lower third of the esophagus.

Risk factors such as extensive use of tobacco and alcohol increase the risk of esophageal cancer significantly, however dietary lifestyle habits, obesity, or injury of the esophagus area can also encourage cancer formation.

Esophageal cancer is one of the most dangerous types of cancer because of its difficulty to be diagnosed. That is due to the absence of any symptoms until it has reached an advanced stage and take up to 60% of the circumference of the esophageal tube. One of the most common symptoms is difficulty or pain during swallowing. The feeling often starts to be mild and is getting more unpleasant over time. This happens since the tumor keeps growing inside the esophagus covering a bigger and bigger area of it (see fig. 2). At some point, even liquids may be hard to be swallowed. As a result, weight loss is also one symptom since it is painful for one to eat. Other symptoms can be chest pain, hoarseness, and chronic cough.

For the treatment procedure, surgery may is applied if it is possible, called esophagectomy. If the tumor is in early stage, endoscopic treatments can be done by passing an endoscope down to the throat and into the esophagus in order to remove the malignant tumor from the

inner layer. Radiotherapy is applied in cases where the patient can not go through a surgery due to poor health or before surgery in order to shrink the tumor, after surgery in order to kill any cancer cells left. In some cases, radiation therapy is being used in palliative therapy to prolong survival. There are two types of radiation therapy, internal beam and external, in this thesis we are working with the later.

Unfortunately, many times radiation therapy is followed by unpleasant side effects such as skin irritation, nausea or fatigue and others. However, modern radiotherapy techniques have been developed trying to minimize them as much possible.

1.1.1 *Tumor position*

The tumor position of esophagus cancer depends on the type of the carcinoma: squamous cell carcinoma or adenocarcinoma. In clinical routines, the position is defined by vertebral column (spine). The spine consists of 33 vertebrae: 24 presacral vertebrae (7 cervical, 12 thoracic, and 5 lumbar) followed by the sacrum (5 fused sacral vertebrae) and the coccyx (4 frequently fused coccygeal vertebrae). The abbreviations C., T., L., S., and Co. are used for these regions [3].

We assigned as ”Upper” position the tumors located within $C_1 - T_4$, as ”Middle” the tumors within $T_1 - T_9$ and finally ”Lower” within $T_9 - L_5$.

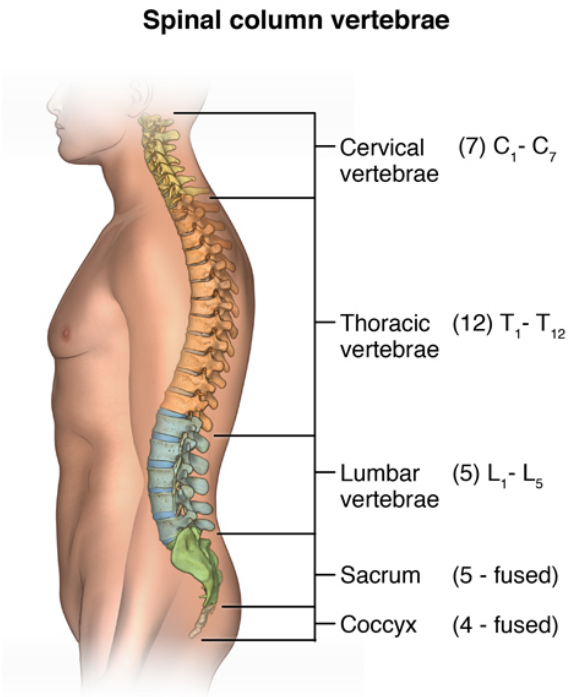

Figure 3: Vertebral column numbers (from Basic human anatomy [3])

1.2 IMAGE GUIDED RADIOTHERAPY

As is being defined, by Timmerman et al. in [1], image-guided radiation therapy is the use of imaging to plan and initiate radiotherapy treatment. While image-guided and adaptive radiation therapy is the on-going use of imaging to monitor, update, and adjust the treatment process. Both techniques have improved the precision and accuracy of the treatment delivery significantly especially for tumors located in areas of the body which are difficult to remain motionless, for example, lung cancer. Image-guided radiotherapy (IGRT) was developed to limit the geometrical uncertainties by acquiring images of the patient's anatomy directly before treatment and comparing these with the anatomy during the treatment planning, by using three-dimension rigid image registration.

1.3 DEFINITION OF VOLUMES

The definition of tumor, target organs as well as organs at risk (OAR) for radiotherapy is vital to its successful execution. The delineation of these volumes is obligatory for the treatment planning process so the absorbed dose to be well defined, prescribed, recorded and reported. As they are defined in the Journal of the International Commission on Radiation Units and measurements (ICRU)[4] the volumes are the following:

- **Gross tumor volume / GTV:** The GTV is the gross demonstrable extent and location of the tumor. The GTV may consist of a primary tumor (GTVp or GTV-T), metastatic regional node(s) (GTVn) or distant metastasis (GTV-M).

- **Clinical target volume / CTV:** The CTV is a volume of tissue that contains a demonstrable GTV and/or sub-clinical malignant disease with a certain probability of occurrence considered relevant for therapy.

- **Planning target volume / PTV:** The PTV is a geometrical concept introduced for treatment planning and evaluation. It is the recommended tool to shape absorbed-dose distributions and ensure that the prescribed absorbed dose will be delivered to all parts of the CTV with a clinically acceptable probability, despite geometrical uncertainties such as organ motion and setup variations.

- **Organ at risk / OAR:** The OAR or critical normal structures are tissues that if irradiated could suffer significant morbidity and thus might influence the treatment planning and/or the absorbed-dose prescription.

- **Planning organ-at risk volume / PRV:** As is the case with the PTV, uncertainties and variations in the position of the OAR during treatment must be considered to avoid serious complications. For this reason, margins have to be added to the OARs to

compensate for these uncertainties and variations, using similar principles as for the PTV. This leads, in analogy with the PTV, to the concept of PRV.

1.4 IMAGE REGISTRATION

Image registration is the process of determining the geometric transformation that relates identical (anatomic) points in two image series: a moving data-set and a stationary source data-set. In other words, image registration aims to find the transformation for mapping the points in the source image into the points in the reference image. Figure 4 shows the four types of image transformations, in this project we worked with rigid and deformable (elastic). Image registration is used in image-guided radiotherapy for treatment planning to ensure accurate patient positioning at the time of treatment. Furthermore, it is used to combine information and delineate tumor volumes between different imaging modalities (MR, PET, CT,..).

1.5 RIGID & DEFORMABLE IMAGE REGISTRATION

The only difference between rigid and deformable registration is the transformation component. Rigid registration considers only translations and/or rotations having a maximum of six degrees of freedom. All pixels move and/or rotate uniformly so that every pixel-to-pixel relationship remains the same before and after transformation. Deformable registration can be described as a rigid registration for each voxel since can include translations and/or rotations for each point having a large number of degrees of freedom. All voxels can move without keeping the pixel-to-pixel relationship the same, resulting in a post-registration image that may have been translated, rotated, re-sized, and stretched.

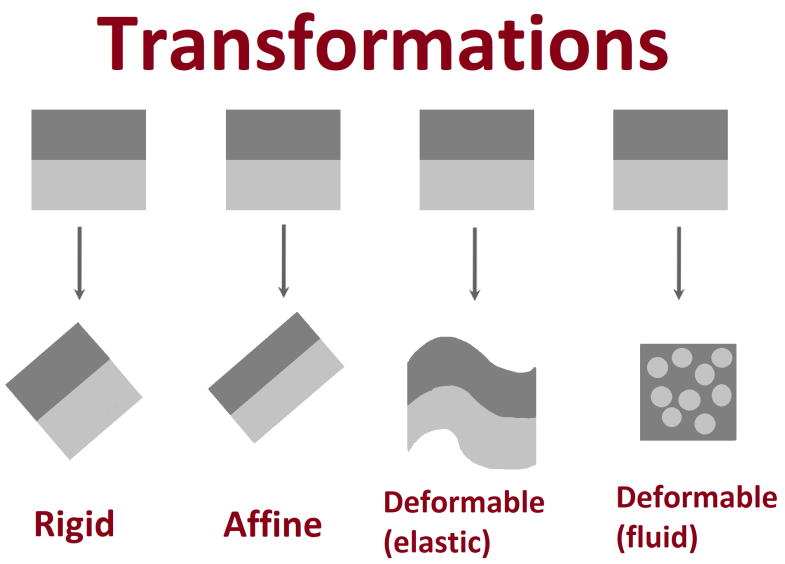

Figure 4: Image registration transformations

1.6 ONLINE VERSUS OFFLINE MATCHING

Online matching refers to the online corrections and adjustments which take place during the treatment session while the patient is lying on the treatment couch. Online corrections could refer to position adjustments of the patient's couch or even further re-optimization of the treatment parameters depending on the anatomical changes that may have occurred. For the online corrections daily pre-treatment scan is taken and if it deviates on any orthogonal axes more than a defined threshold from the treatment planning image then online corrections are performed. Online corrections can control random set-up errors, but most importantly minimize systematic errors that have a larger impact in the margin calculation. In addition to these, online match benefits patients with significant anatomical changes during the treatment course as well as with target volumes defined critically close to high-risk organs.

Offline matching refers to offline post-treatment corrections and adjustments. Offline corrections are based on images acquired during previous fractions and as a result, can only affect improvements on systematic set-up errors.

Both online and offline image-guided correction strategies aim to minimize the geometric

set-up uncertainties by reducing any variations between the treatment planning images and the daily pre-treatment scans. There are two components to set-up error, those being systematic and random. A systematic error can be defined as an error that is introduced at the planning stage and, if unaddressed, would occur and effect for each treatment fraction. A random error occurs only once and as the name implies is unpredictable. They are treatment execution errors and they are having a different effect at different treatment fractions. As a result, the systematic errors will move the delivered dose distribution whereas the random errors will blur it.

Part II

METHODOLOGY

2

RIGID IMAGE REGISTRATION

To investigate the first aim of the thesis, 20 consecutive patients with oesophageal cancer were retrospectively selected from the treatment-planning database. All patients underwent curative treatment at Rigshospitalet in 2017, with a total treatment dose of 50 Gy given in 25 fractions. Each patient had been scanned daily with cone-beam CT (CBCT) for image guidance, resulting in 25 CBCT scans per patient. Following the privacy policy, all the patients had been anonymized and no relevant detail revealing their identity was available. In this study, we re-registered 6 out of 25 CBCTs per patient (nr. 1, 5, 10, . . . 25) with focus on three different structures: bones (primarily the spine), gross tumor volume (GTVp), and clinical target volume (CTV). Image registrations were performed rigidly in Aria platform, Image Registration (by Varian Medical Systems inc.). In the Aria platform, the Image Registration environment when a specific patient is loaded into the system looks like the following picture (see fig.5). In the figure, we can see all the 25 daily pre-treatment images taken during each fraction. Each white line connecting each CBCT to the plan treatment CT indicates the online rigid image registration which performed right before the treatment procedure and it is mainly an image registration focused on the spine. In the last two buttons, there are also visible the treatment planning CT and PET scans. The plan treatment CT is the one that contains all the normal tissue and tumor target volumes contouring, done by radiation oncologists. (see fig. 6).

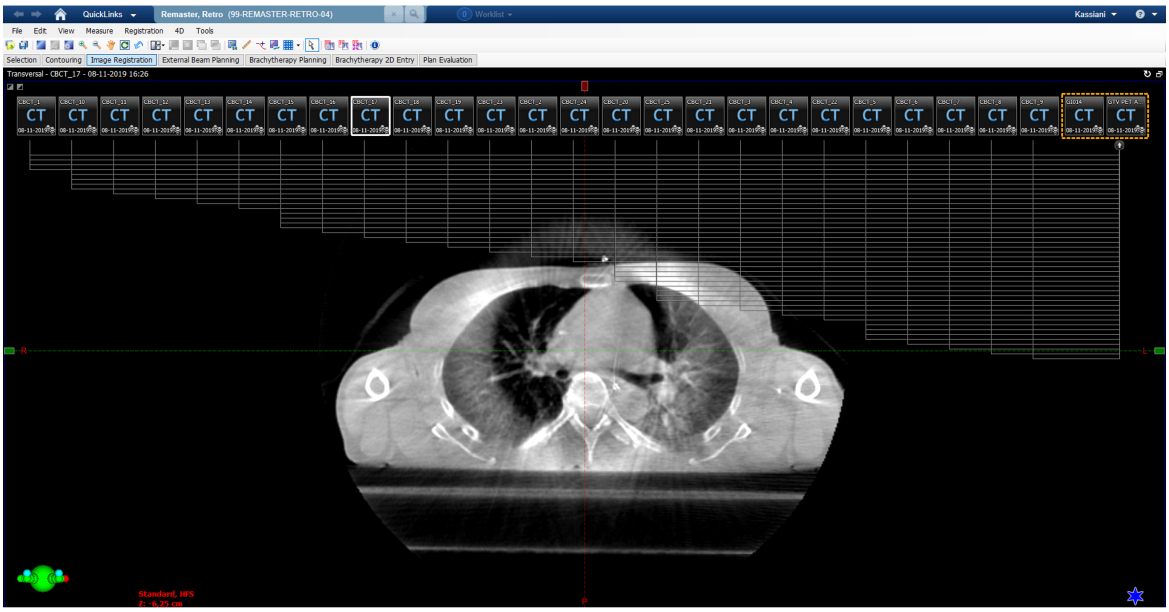

Figure 5: Example of the daily pre-treatment CBCT scans.

The CT and the contours are visible in three different view angles (fig.6): transversal, sagittal & coronal giving a very good overview of the patient's area of interest. The structures that have been drawn on the scan are: bone/body (green), couch interior and surface (magenta), GTV primary and nodes (red), CTV (orange), PTV (cyan), lungs (blue) and spinal cord and PRV spinal cord (magenta as well). It is easy to observe the huge image quality difference between the CBCT and the CT scans.

Since the offline rigid image registration performed using the auto-match selection, there was limited control of the software's actions. Our contribution was to place the red box carefully so it encompasses the volume of interest each time. It was needed to check all three view angles as well as across all CT slices, that our region of interest was lying inside the red box's volume. Since each time we were focused on a different structure, we had to place the red box accordingly. The following images show the procedure.

As we can observe in figures 7, 8 & 9 it helps to have visible only the structure we are interested in each time, we can choose what we see from the list with the structures on the left. The bone structure is with green color (fig. 7), the GTV with red (fig. 8) and CTV with orange (fig. 9). At this point, we need to mention that all the image registrations performed in

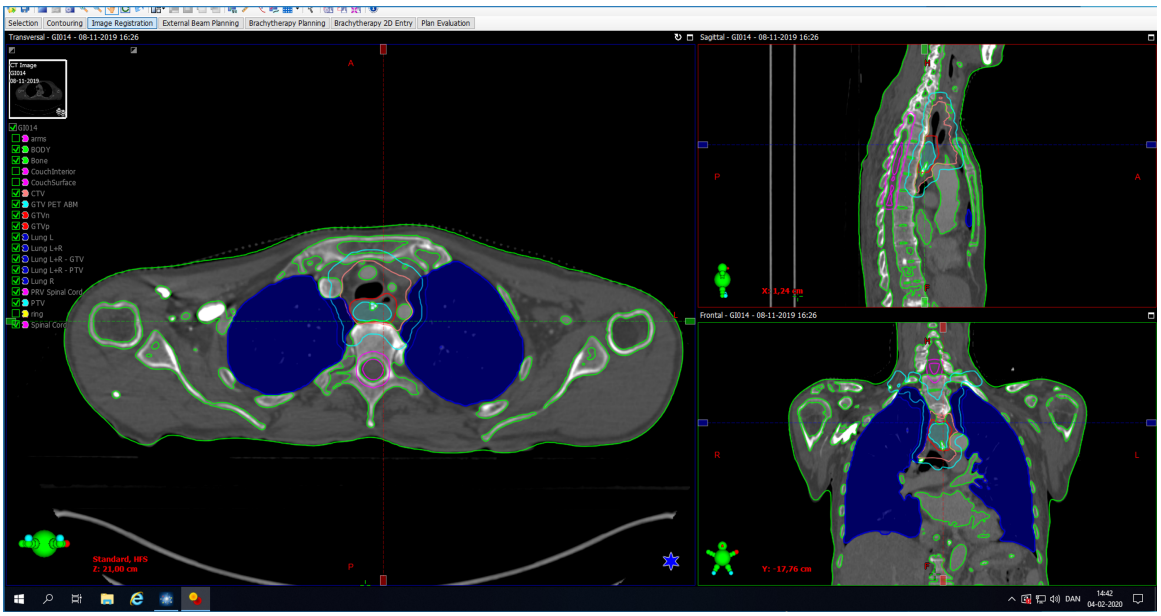

Figure 6: Plan treatment CT image with target and organs at risk delineations marked with different colors.

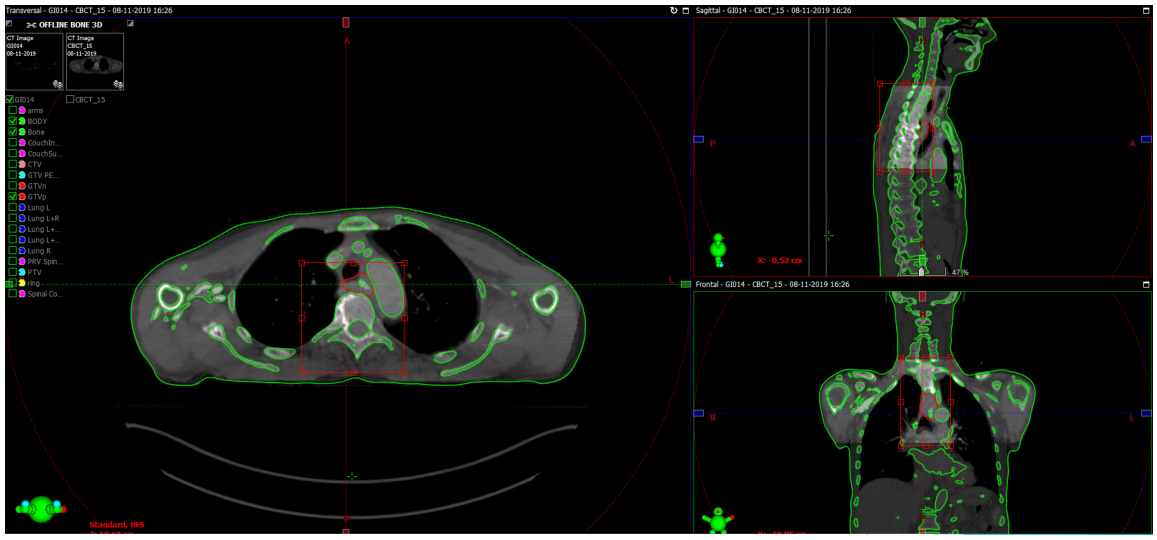

Figure 7: Rigid registration with ROI encompassing the spine.

3D and we did not take into account rotational corrections in ”pitch” and ”roll” direction . To improve the quality of the registration and in some cases prevent the rigid image registration algorithm from failing, it is important the volume of interest to include only the structure we are focused on as much as possible, avoiding other structures. This way the best result for the image registration could be achieved. We could consider image registration with respect to bones (spine), for example as in fig. 7. Taking a wider ROI encompassing also part of the

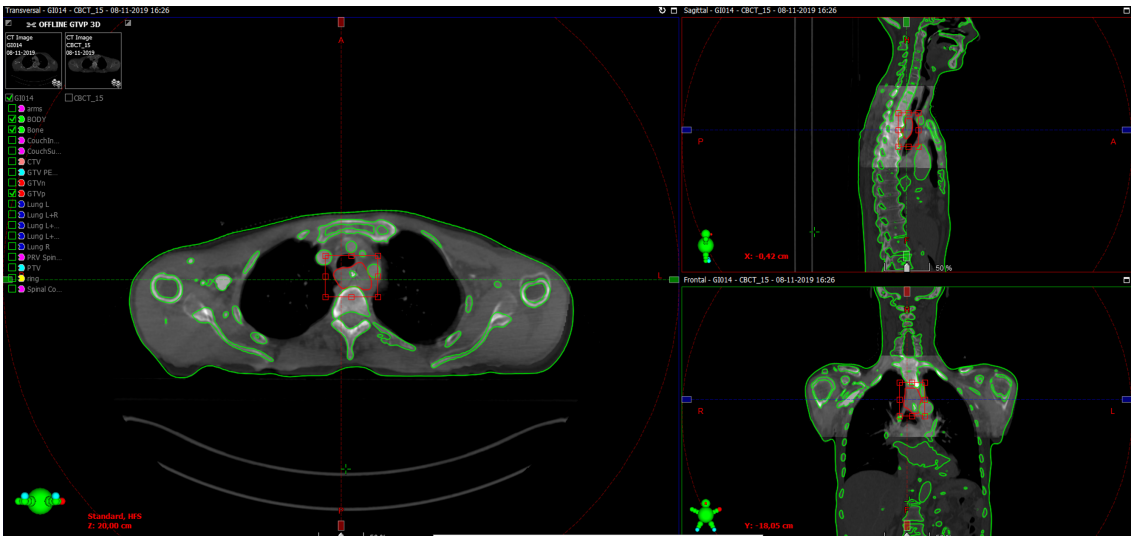

Figure 8: Rigid registration with ROI encompassing the GTV.

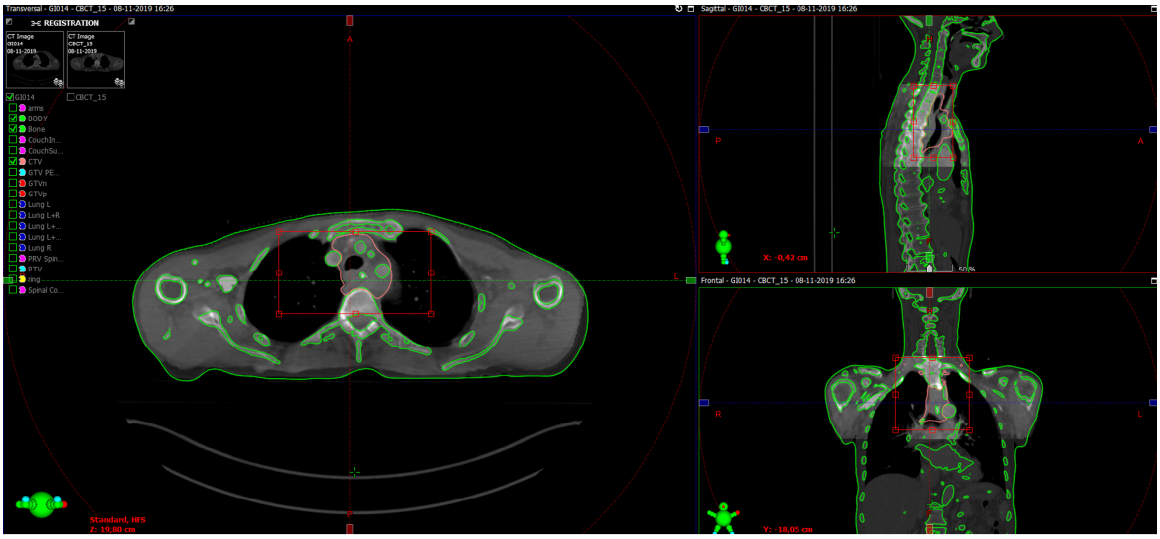

Figure 9: Rigid registration with ROI encompassing the CTV.

shoulder bones might lead to low-quality image registrations since shoulders and arms are hard to place in the exact same position as it was when the plan treatment CT was taken.

Finishing the procedure image rigid registration procedure for all patients, we have three different image registration techniques for five out of twenty-five CBCTs for each patient. From software we can retrieve details for each registration we performed, the information we are interested in is the translational coordinates. By right-clicking on the white lines and tapping on ”Properties” we get the following window:

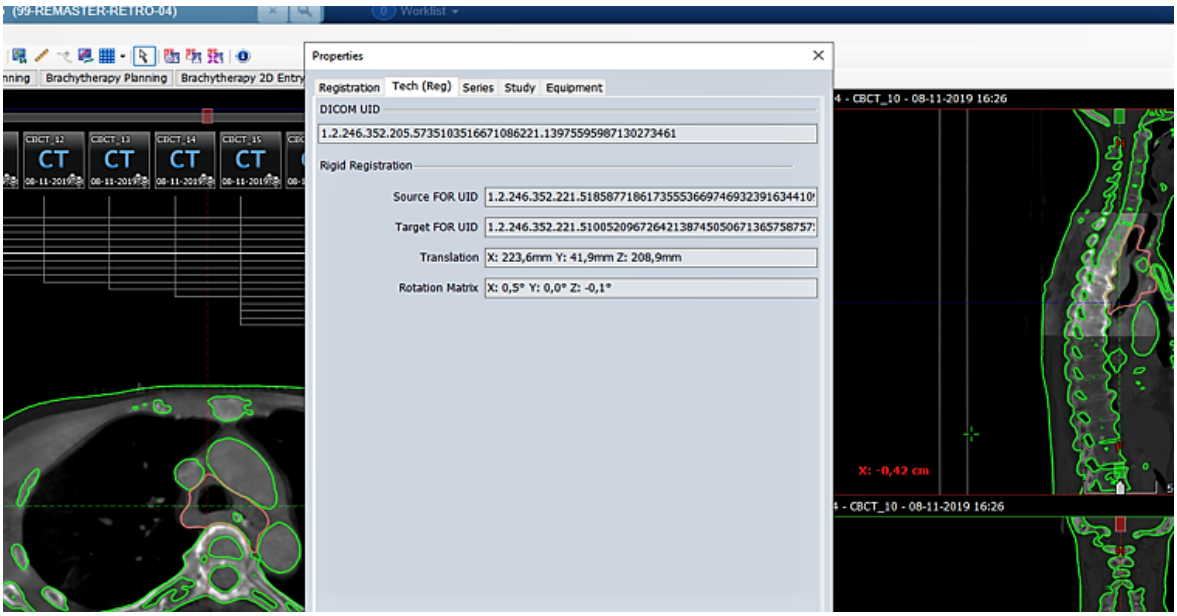

Figure 10: Translational coordinates of current rigid image registration.

In the ”Properties” window, under the tab ”Tech (Reg)” we can collect the 3D translation coordinates in millimeters. Figure 27 in the Appendix section, shows how the difference in the matching of the planning CT and a CBCT during the RIR procedure look like while we focus on ”soft tissue” match, specifically on CTV.

In the ”Results” part of the thesis, we present the data of the translational coordinates collected from the rigid image registration procedure as well as the systematic and random errors of the image registration procedure. This part of the thesis aims to compare the different registration methods we applied and figure out if a specific method is more suitable for each case of the tumor position and how much the methods deviate from each other. Gathering all the data in an Excel file we analyze them with the use of python script written for this purpose. This was applied for each patient, each CBCT, and for all coordinate directions individually. For each patient then we conclude to tables which contain the result of the subtractions for the three different comparisons, namely ”Bone-GTV”, ”Bone-CTV” & ”GTV-CTV”. In new tables, one for each comparison, we gather the results of the mean and the variance across all six CBCTs for each patient and anatomical direction in order to calculate the systematic and random uncertainties. Using the van Herks formula, we performed margin calculation for

bone match under ”perfect soft tissue match” assumption. To examine how much the three groups deviate from each other, we applied statistical analysis and in our case specifically, we used the ”One sample t-test”. The one-sample t-test determines whether the sample mean is statistically different from a known or hypothesized population mean. In our study, the null hypothesis (H_0) and the alternative hypothesis (H_1) of the one sample t-test can be expressed as:

- H_0: $\mu = x$ where the sample mean is equal to the hypothetical population mean
- H_1: $\mu \neq x$ where the sample mean is not equal to the hypothetical population mean

where x is the hypothetical number for the population mean and μ is the sample mean. Our hypothesized population mean is $x = 0$, meaning that the testing image registration strategies do not deviate with each other. For the null hypothesis to be rejected, an observed result has to be statistically significant, in other words the observed p-value to be less than 0.05. We, also tested the human error during the image registration procedure and for this reason, we repeated the procedure one more time for five out of twenty patients and three out of six CBCTs which they were randomly chosen with a random generator algorithm.

3

DEFORMABLE IMAGE REGISTRATION

In a further investigation, we want to examine the treatment quality with respect to the dose coverage over the treatment period (on average 25 days). It is highly likely that anatomical changes may occur during the 25 days interval. we want to examine in what extend the current clinical workflow works well under different situations and if indeed prevents any incomplete dose coverage of target. Furthermore, we want to test how the different rigid registration strategies affect the dose distribution. In order to probe this, we used raw and processed (rigid registrations) data from the first aim. Due to the time limitation, we studied randomly 3 out of 20 patients. The software used was the Aria and Velocity platform (by Varian Medical Systems inc.). To examine the anatomical changes over the treatment period we deformed the planning CT anatomy to the current CBCT anatomy and as a next step, we also deformed the original structures of the CT to the newly adapted CT.

In the Velocity platform as we can see in figure 11, there is the list with all daily scans and treatment planning CT on the left. We are allowed to load at the same time two volumes, so each time we opened the current CBCT as the primary volume (since is the volume which will guide the planning CT how to be deformed) and the planning CT as the secondary volume.

The next step is to choose a rigid registration strategy in order to register these two volumes (fig. 12) and then the program proceeds to the deformable registration. For the rigid

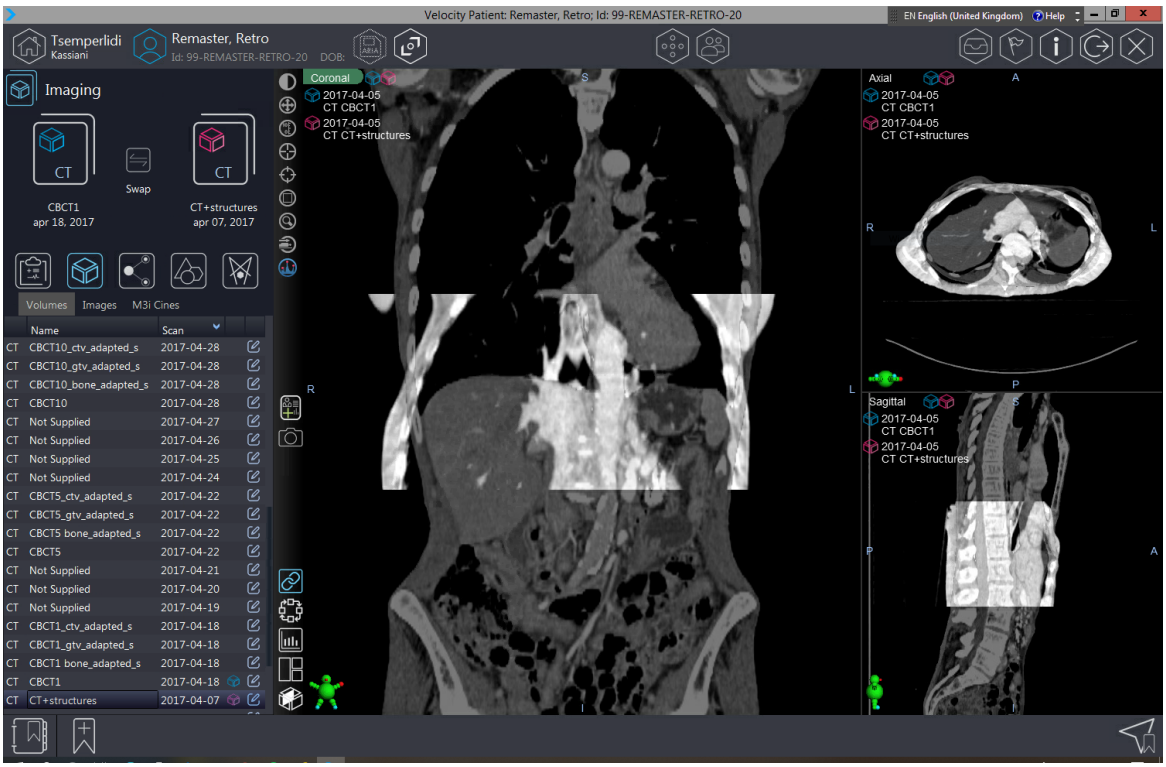

Figure 11: Planning CT and CBCT on top of each other, non registered volumes

registration, we applied the exact same ones as we performed them in aim 1, the software allowed us to load them without the need of performing them again.

The resulting volume is the original planning CT but with the anatomy changed in the registered with CBCT area. This new volume is called ”adapted CT” and one can distinguish the adapted area at the points where the red arrows indicate (see fig. 13). We repeated all these steps testing all 3 registration strategies (Bone, GTV & CTV) on the same 6 out of 25 CBCTs in total per patient as in the first part of the project.

Since the adapted CT has different anatomy from the planning CT, we should not use the original structures in order to test the dose coverage because we are going to get misleading results in the dose-volume histogram. For that reason, in Velocity platform we follow the steps of the guided navigator and we choose the ”Segmentation” tab and next the ”Structure Deformation”. Following the steps, we end up with deformed structures that match the anatomy of the adapted CT. It is noteworthy that we have to make sure that through all the

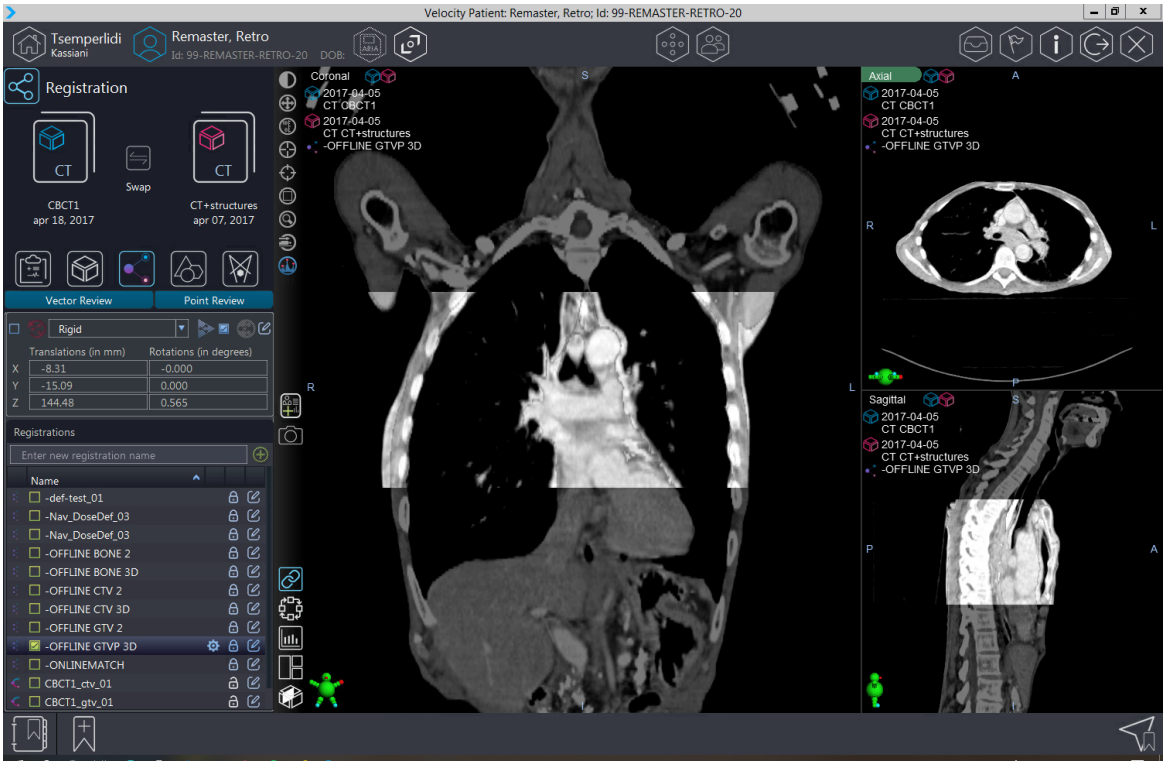

Figure 12: An example of planning CT and CBCT rigidly registered with bone match.

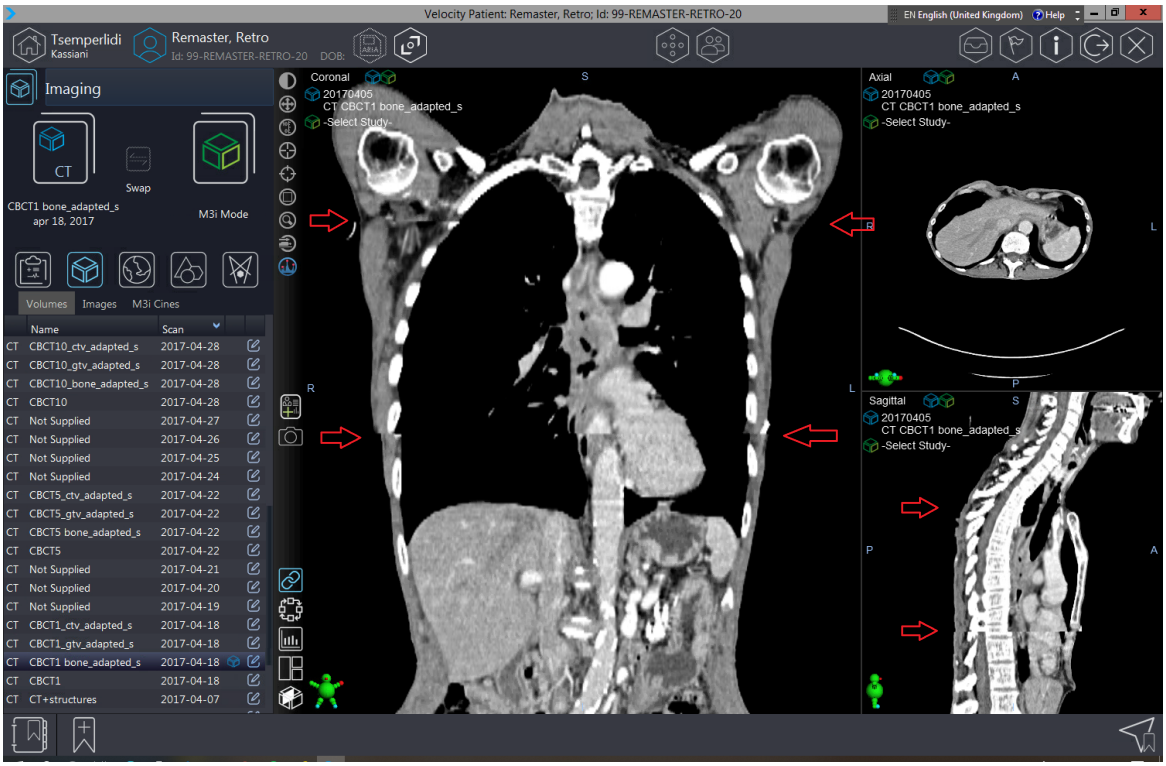

Figure 13: By the end of deformation process we get the ”Adapted CT”.

slices, especially in the adapted area the new structures are very well defined and reasonable and they match with the picture anatomy as we see it, otherwise our results and conclusions will be affected negatively.

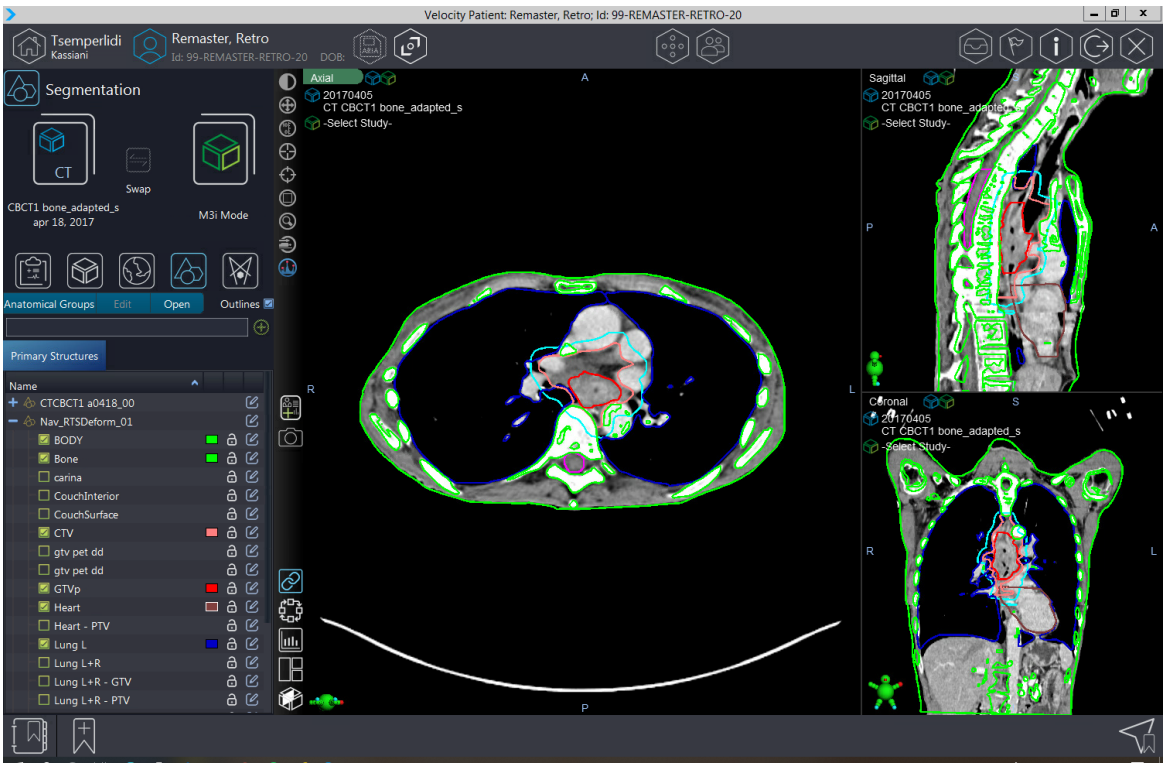

Figure 14: Adapted CT with the deformed structures.

As final step, we transfer all our adapted CTs to Eclipse platform and we mainly work in the ”External Beam Planning” section where we copy the original dose used for the treatment and paste it each time to our current CT. It is vital to ensure that all settings used for the calculation of treatment dose, are the exact same when we paste and recalculate the dose on the adapted CTs. To compare the effects of the anatomical changes as well as of the different registration strategies on the treatment progress, we plot dose-volume histograms (DVH) focusing on the PTV coverage. The histograms are shown in the ”Results Part II” section.

Part III

RESULTS

4

RESULTS PART I

4.1 REPRODUCIBILITY OF RIGID REGISTRATIONS

As mentioned in ”Methods” section, we investigated the producibility of our results, repeating the RIR procedure once again for five out of twenty patients and for three out of six CBCTs which they were randomly chosen with a random generator algorithm.

	Direction	**SD**	**Range**
Bone	**LA**	6.6	0.0 - 17.6
	AP	4.5	0.0 - 14.2
	SI	9.4	0.0 - 26.2
GTV	**LA**	6.7	0.0 - 19.0
	AP	5.6	0.1 - 16.7
	SI	9.6	0.0 - 27.7
CTV	**LA**	8.3	0.1 - 25.3
	AP	6.9	0.0 - 21.3
	SI	10.2	0.0 - 27.0

Table 1: Results of reproducibility of RIR in millimeters.

The SD of reproducibility ranges between 4.5 up to 10.2 mm, the biggest standard deviation and range appear to be for the superior-inferior direction in all three cases. Range values gives us a better overview of the variation of our data even in the case where SD seems satisfying.

4.2 DIFFERENT IMAGE REGISTRATION STRATEGIES

4.2.1 *Bone-GTV & Bone-CTV*

Following the guidelines of the margin formula from van Herk et al paper [6] we calculate the PTV margin which is required to provide 95% dose coverage of 90% of the patients. α is a constant and its specific value for 90% confidence in 3D is 2.5, the numerical value of β for the 95% isodose surface is 1.64 and γ is equal to 0.7. Σ is the combined standard deviation (SD) of all preparation error (systematic) whereas σ represents the quadratic sum of the SD of all treatment execution (random) variations (organ motion and setup error) including the SD describing the penumbra (σ_p), σ' is the combined standard deviation of treatment execution (random) variations excluding the penumbra.

$$m_{PTV} = \alpha\Sigma + \beta\sigma - \beta\sigma_p = \alpha\Sigma + \gamma\sigma' \tag{1}$$

Table 2 shows the values for systematic and random errors while table 4 shows the final results for PTV margins, both tables given in millimeters. The uncertainties were calculated as the SD of the means for systematic uncertainties and as the root mean square for random.

	Systematic (Σ)			**Random (σ)**		
	LA	AP	SI	LA	AP	SI
Bone-GTVp	2.4	2.1	3.5	4.2	4.6	4.9
Bone-CTV	2.1	2.3	2.1	3.1	3.3	4.3

Table 2: Systematic and Random Uncertainties given in millimeters. The abbreviations stand for the anatomical directions, lateral (LA), anterior-posterior (AP), and superior-inferior (SI).

We observe that systematic uncertainties are smaller than random, which is preferable since the systematic are the ones that have a larger impact on the accuracy of the absorbed

dose delivered to the patient than the random ones. For further analysis, below we have a histogram for each strategy pair in three dimensions (figure series 15). For all histograms the total number of observations on y-axis is equal to 120 (since we studied 6 CBCTs for 20 patients).

Furthermore, to check if there is any specific trend for the different tumor positions, we plotted histograms with different colors having the data grouped by the position. The table 3 shows the number of patients having the tumor located in a specific position along the esophagus.

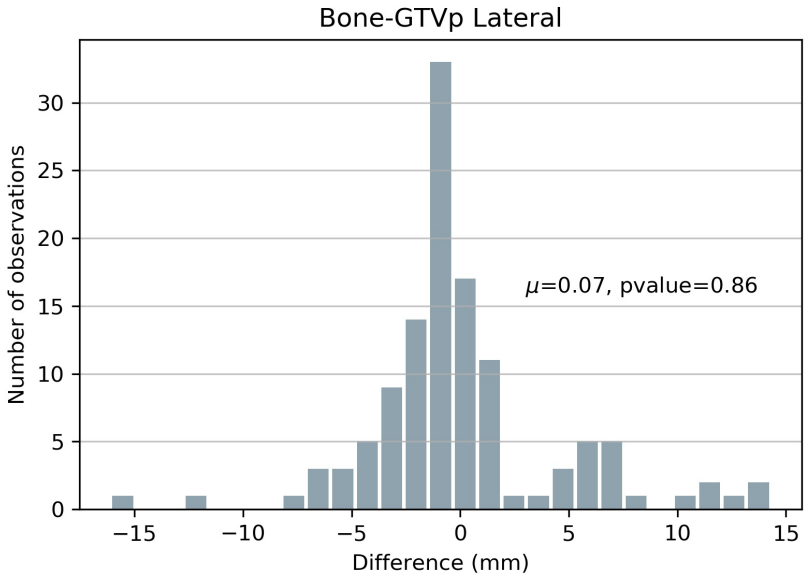

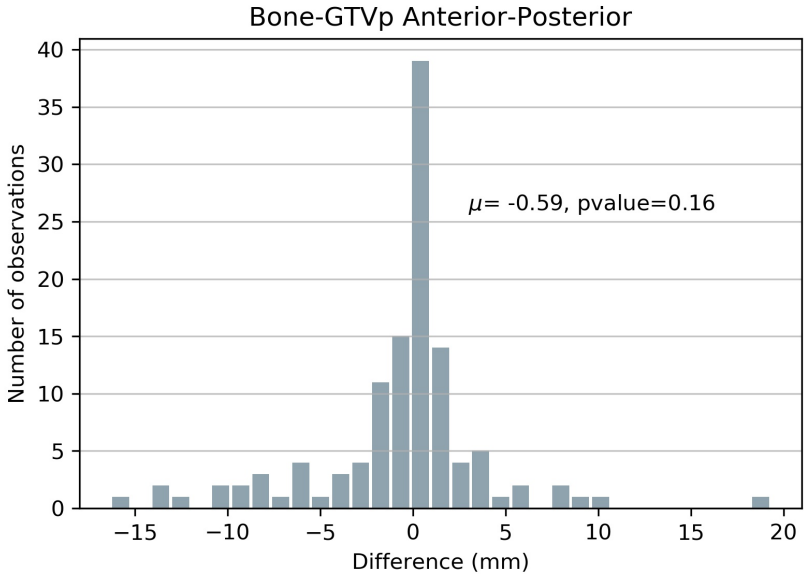

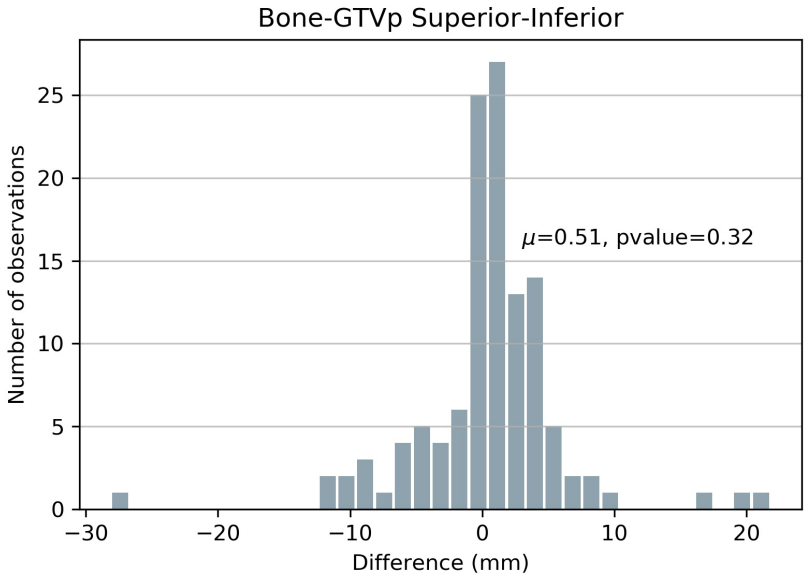
Bone-GTVp Superior-Inferior
Number of observations
Difference (mm)
μ=0.51, pvalue=0.32

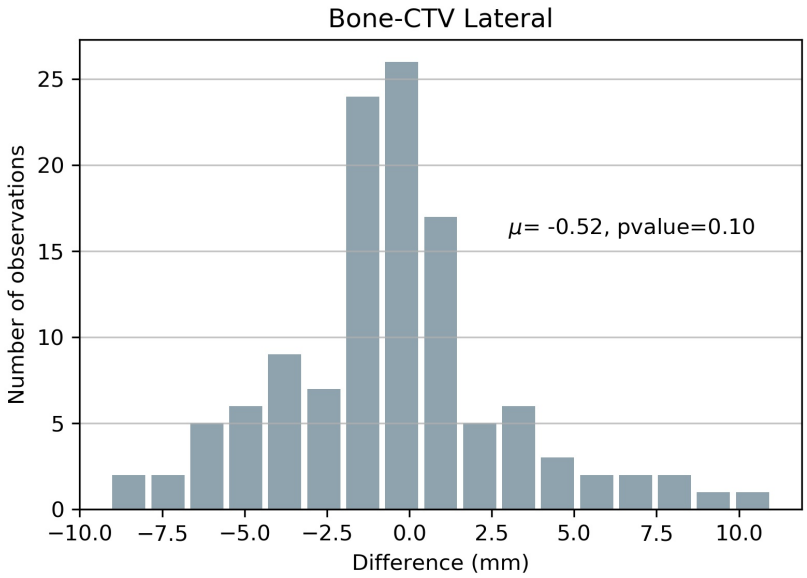
Bone-CTV Lateral
Number of observations
Difference (mm)
μ= -0.52, pvalue=0.10

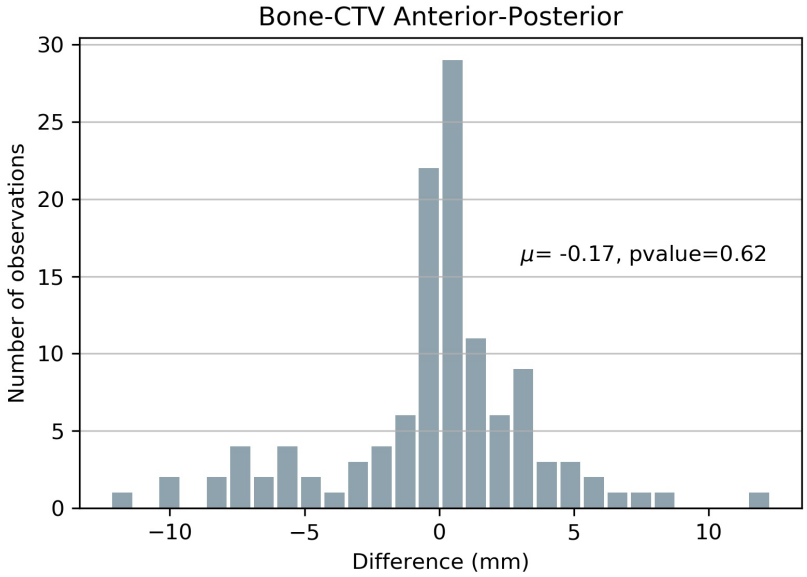
Bone-CTV Anterior-Posterior
Number of observations
Difference (mm)
μ= -0.17, pvalue=0.62

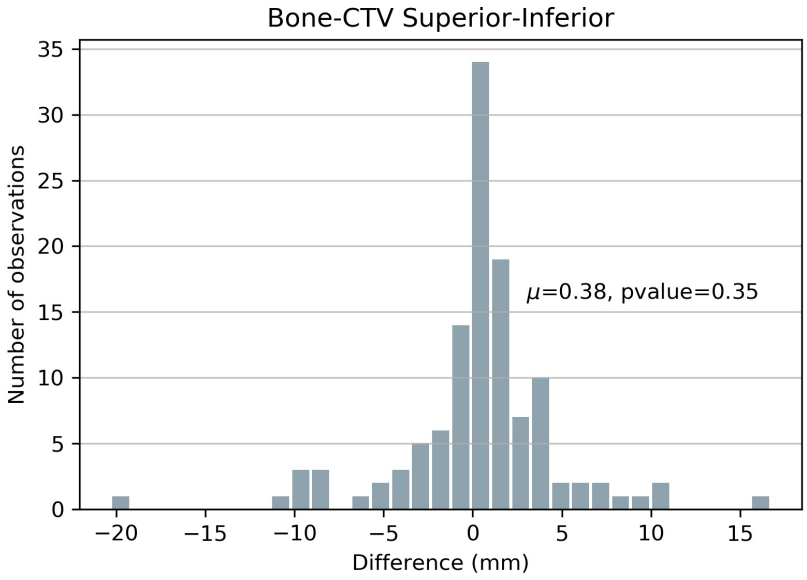

Figure 15: Different RIR strategies difference in each direction.

Number of patients	**Position**
5	Upper
9	Middle
6	Lower

Table 3: Number of patients having the tumor located in a specific position along esophagus.

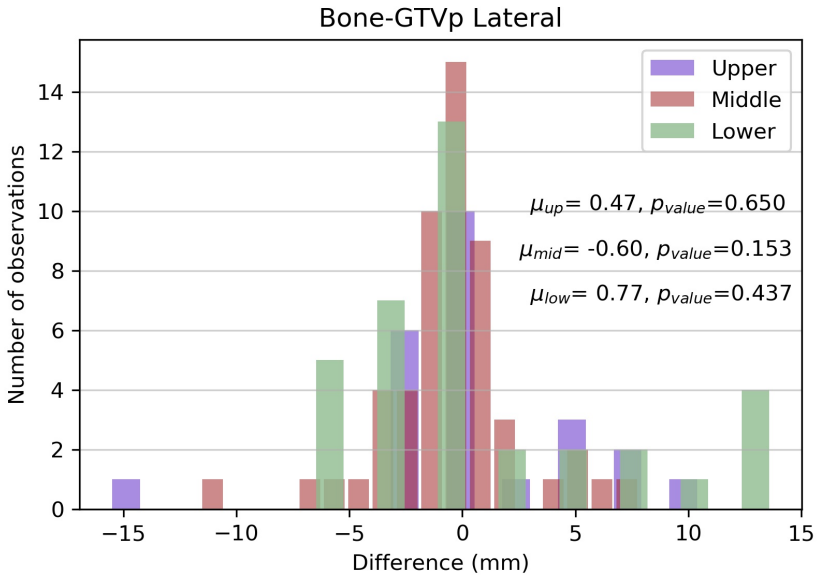
Bone-GTVp Lateral
Upper
Middle
Lower
μ_{up}= 0.47, p_{value}=0.650
μ_{mid}= -0.60, p_{value}=0.153
μ_{low}= 0.77, p_{value}=0.437
Number of observations
Difference (mm)

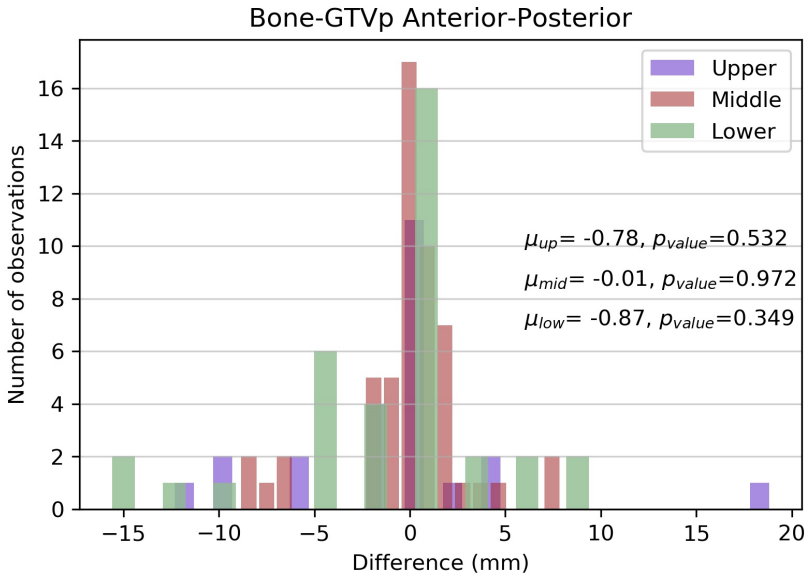
Bone-GTVp Anterior-Posterior
Upper
Middle
Lower
μ_{up}= -0.78, p_{value}=0.532
μ_{mid}= -0.01, p_{value}=0.972
μ_{low}= -0.87, p_{value}=0.349
Number of observations
Difference (mm)

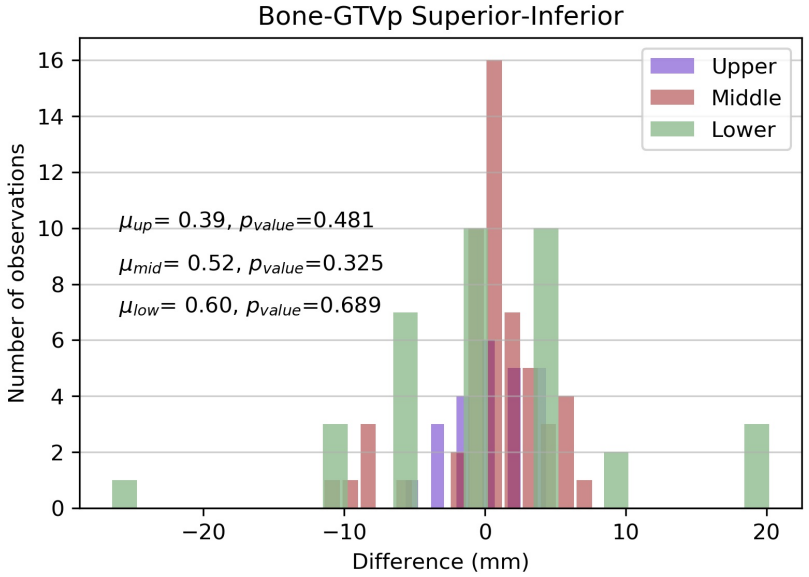
Bone-GTVp Superior-Inferior
Upper
Middle
Lower
μ_{up}= 0.39, p_{value}=0.481
μ_{mid}= 0.52, p_{value}=0.325
μ_{low}= 0.60, p_{value}=0.689
Number of observations
Difference (mm)

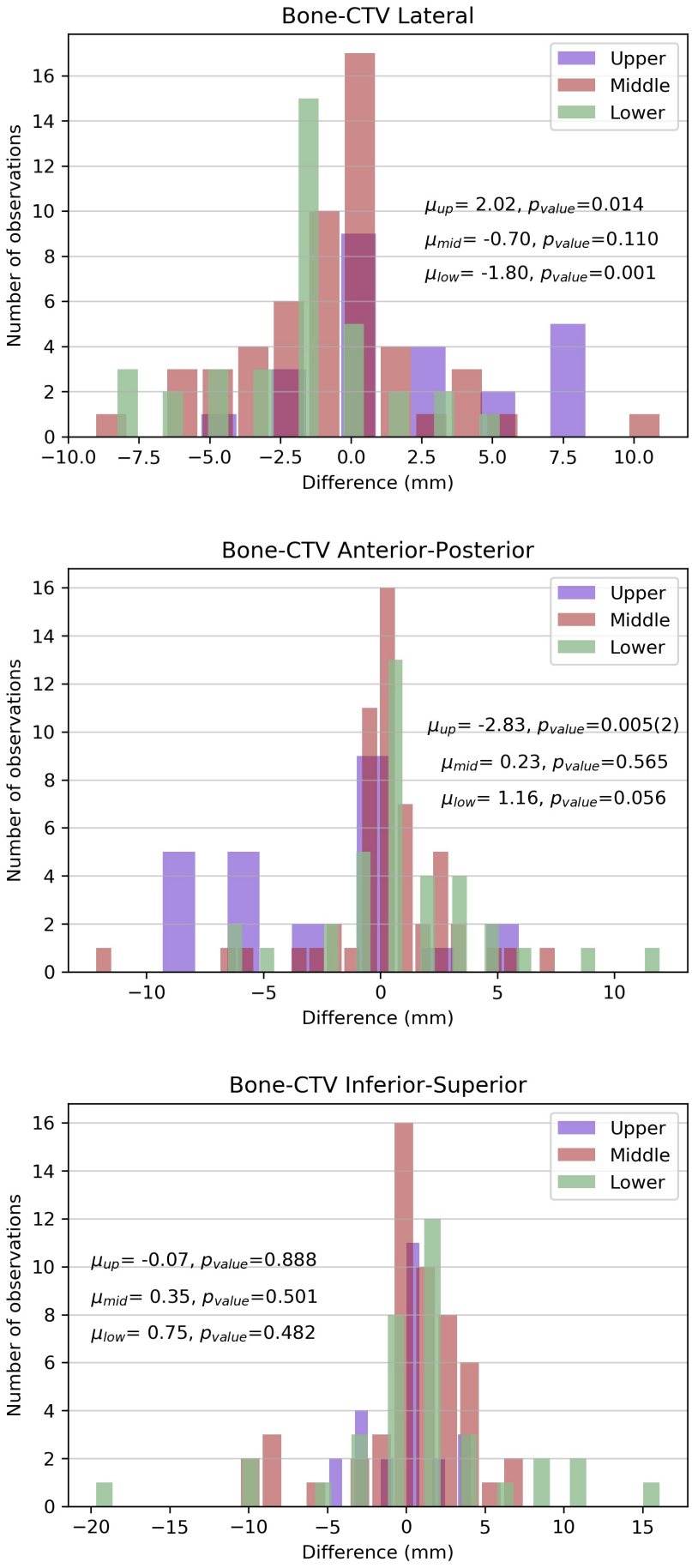

Figure 16: Different RIR strategies difference according to tumor position.

Table 4 includes our results on PTV margin calculation, all numbers are given in millimeters. In the clinical routine, we use bone match strategy with a 7mm CTV-to-PTV margin. In

PTV Margins (mm)					
Bone-GTVp			**Bone-CTV**		
LA	AP	SI	LA	AP	SI
8.98	8.48	12.18	7.38	7.93	8.25

Table 4: Results of PTV margins in mm

this project, we examined what the bone match margins would be if we match in soft tissue instead of bony structure. For example, Bone-GTVp margins, describes the PTV margins assuming that our ground truth is the GTVp match. With a first look we see in Table 4 that in both cases (Bone-GTVp & Bone-CTV) the values are higher than 7mm.

These three correlation scatter graphs below shows the relation between the two registration comparisons, in LA and AP directions clearly there is low correlation. However in SI direction they show higher agreement. These correlation plots (figures 17) as well as the outliers in the histogram plots (figure series 15) confirm that our assumption of ”perfect soft tissue match” does not hold.

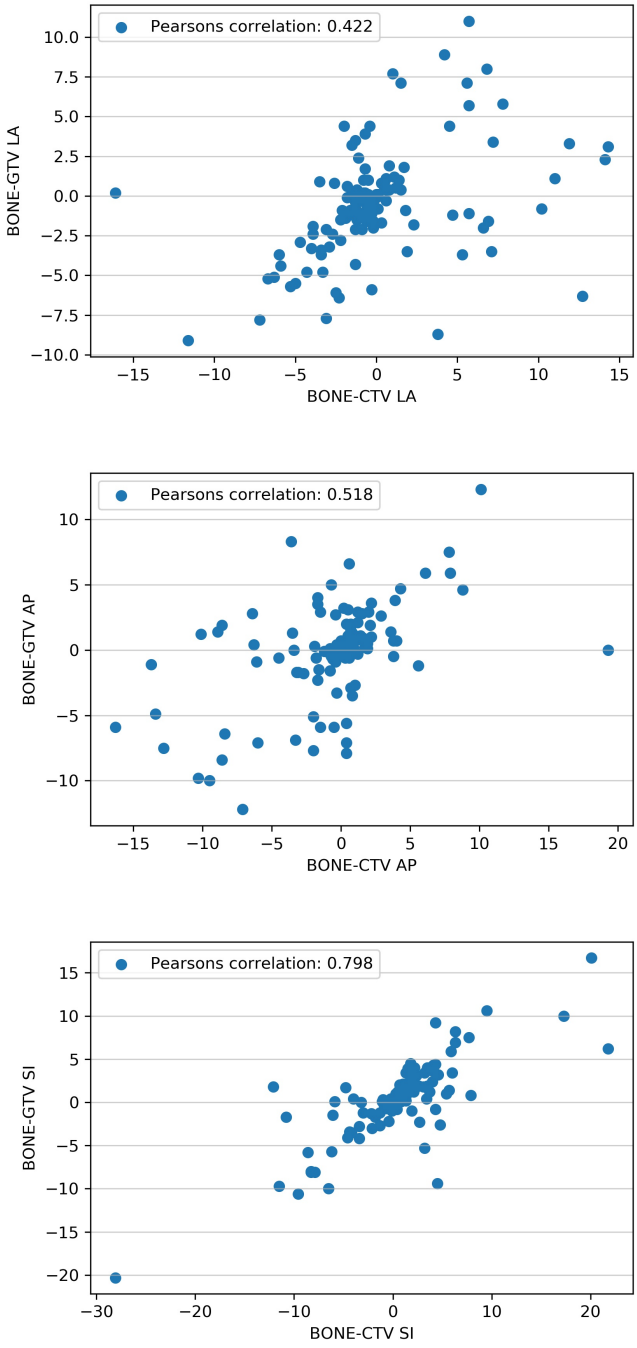

Figure 17: Correlation scatter plot

4.2.2 *GTVp-CTV*

Table 5 shows the values for systematic and random uncertainties resulting for the difference between a GTVp and CTV match strategy. There is a similar trend with the two previous strategies (Bone-GTVp & Bone-CTV) where random uncertainties were larger than systematic.

	Systematic (Σ)			**Random** (σ)		
	LA	AP	SI	LA	AP	SI
GTVp-CTV	2.5	2.1	2.4	4.0	4.0	2.7

Table 5: Systematic and Random Uncertainties given in millimeters.

The figure series 18 are in agreement with the conclusions from figure 17, especially in LA and AP direction there is a significant number of outliers proving that once again our hypothesis on ”perfect soft tissue match” does not hold.

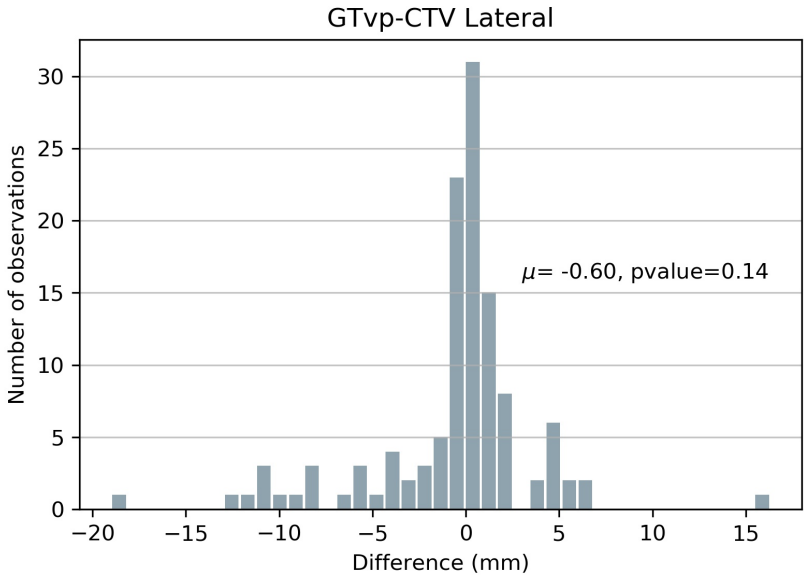
GTvp-CTV Lateral
Number of observations
Difference (mm)
μ= -0.60, pvalue=0.14

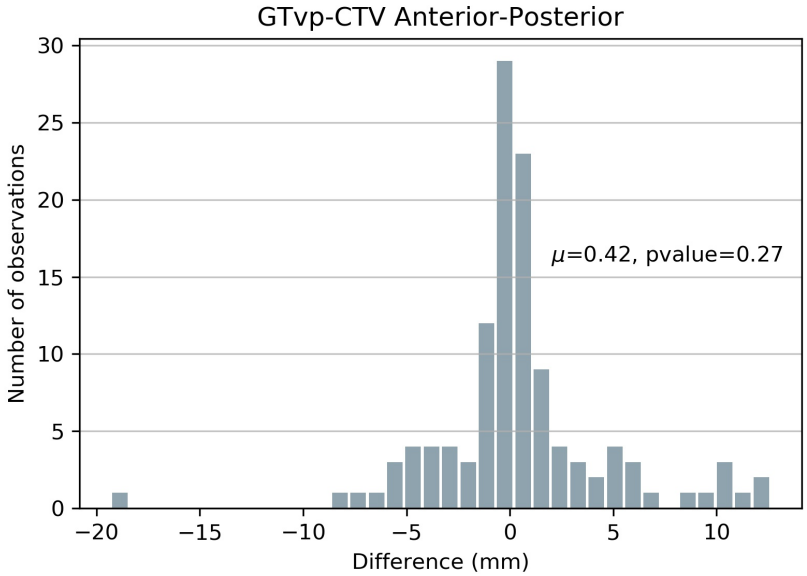
GTvp-CTV Anterior-Posterior
Number of observations
Difference (mm)
μ=0.42, pvalue=0.27

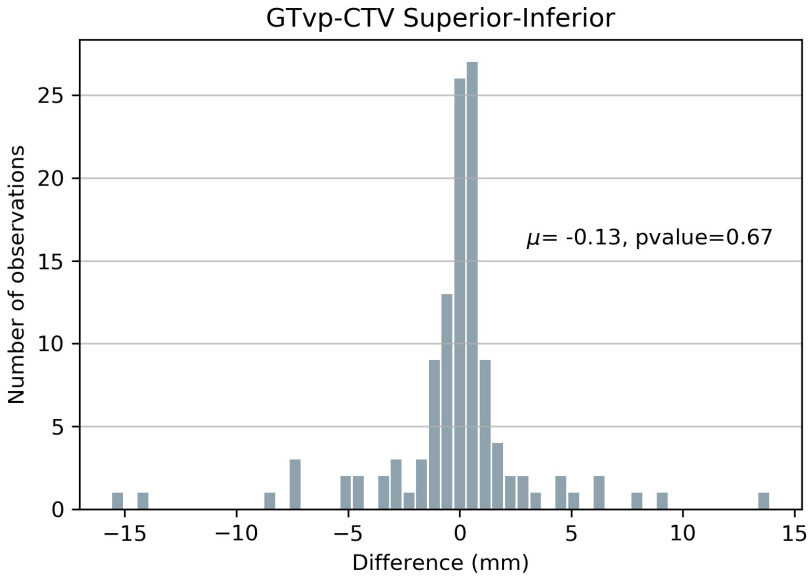
GTvp-CTV Superior-Inferior
Number of observations
Difference (mm)
μ= -0.13, pvalue=0.67

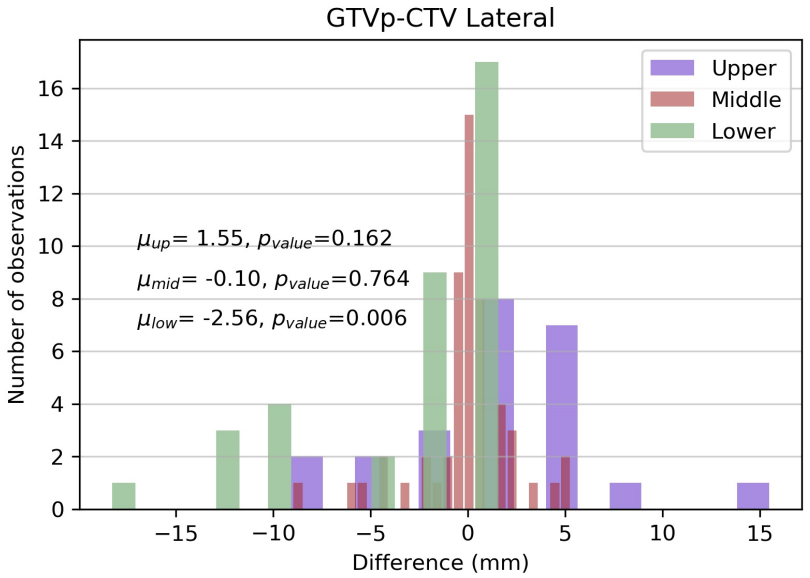
GTVp-CTV Lateral
Number of observations
Difference (mm)
Upper
Middle
Lower
μ_{up}= 1.55, p_{value}=0.162
μ_{mid}= -0.10, p_{value}=0.764
μ_{low}= -2.56, p_{value}=0.006

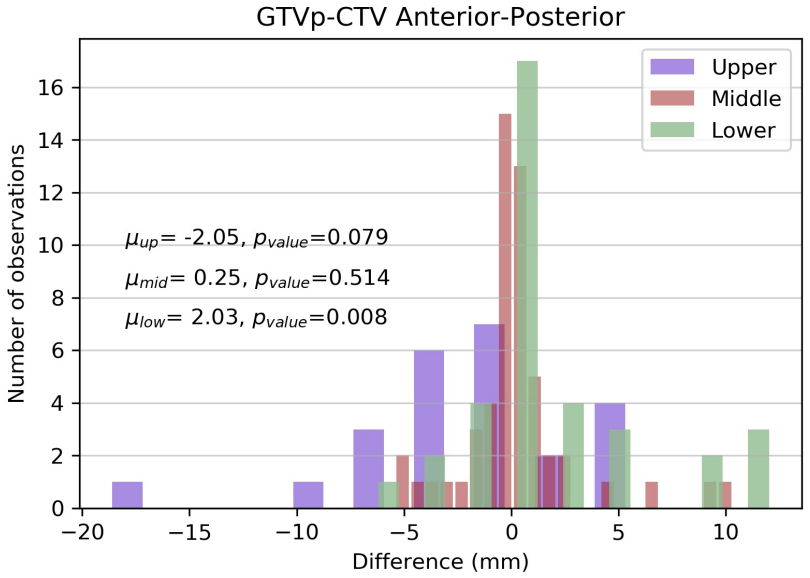
GTVp-CTV Anterior-Posterior
Number of observations
Difference (mm)
Upper
Middle
Lower
μ_{up}= -2.05, p_{value}=0.079
μ_{mid}= 0.25, p_{value}=0.514
μ_{low}= 2.03, p_{value}=0.008

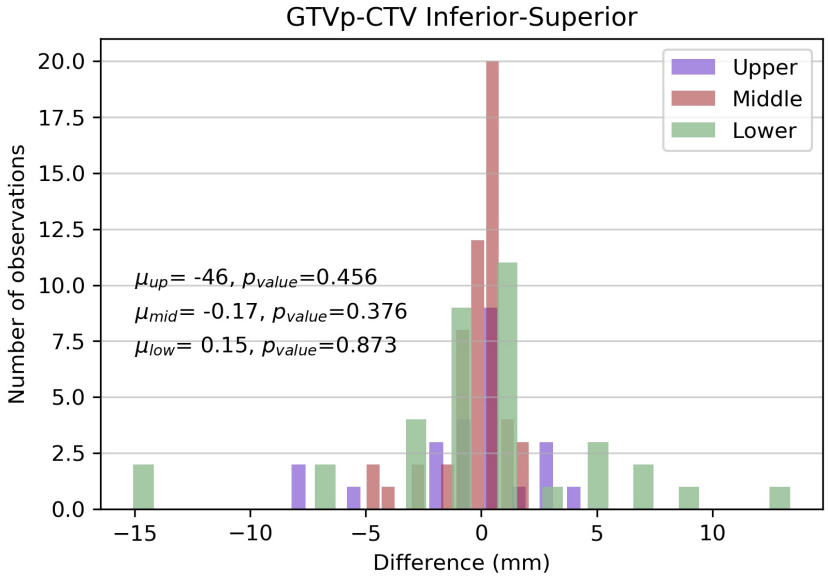

Figure 18: GTVp-CTV strategy difference in three directions.

5

RESULTS PART II

5.1 DIFFERENT IMAGE REGISTRATION STRATEGIES

Gathering the data from the dose-volume histograms, we demonstrate the comparison between the three individual image registration strategies we tested. Each of the following dose volume histograms represents a different patient. We have studied the effect of the registration strategies on 6 out of 25 CBCT as we have mentioned in the Methodology section. Here we show only the first adapted CBCT and the rest can be found in the Appendix.

- Patient 1:

  This patient had only the primary tumor and no nodes had been delineated, the tumor was located in the middle since it was within the thoracic vertebrae. The following DVH graphs (see fig.19) represent the achieved dose coverage on CTV structure calculated for the first CBCT (i.e. first day of treatment.) The square symbol indicates the original dose plan (”GI014 0-50”) on treatment planning CT, the next closest is the dose distribution for the bone match (triangle symbol), the circle and dot symbols represent the dose distributions when we perform rigid image registration focusing on soft tissue, on GTV and CTV respectively.

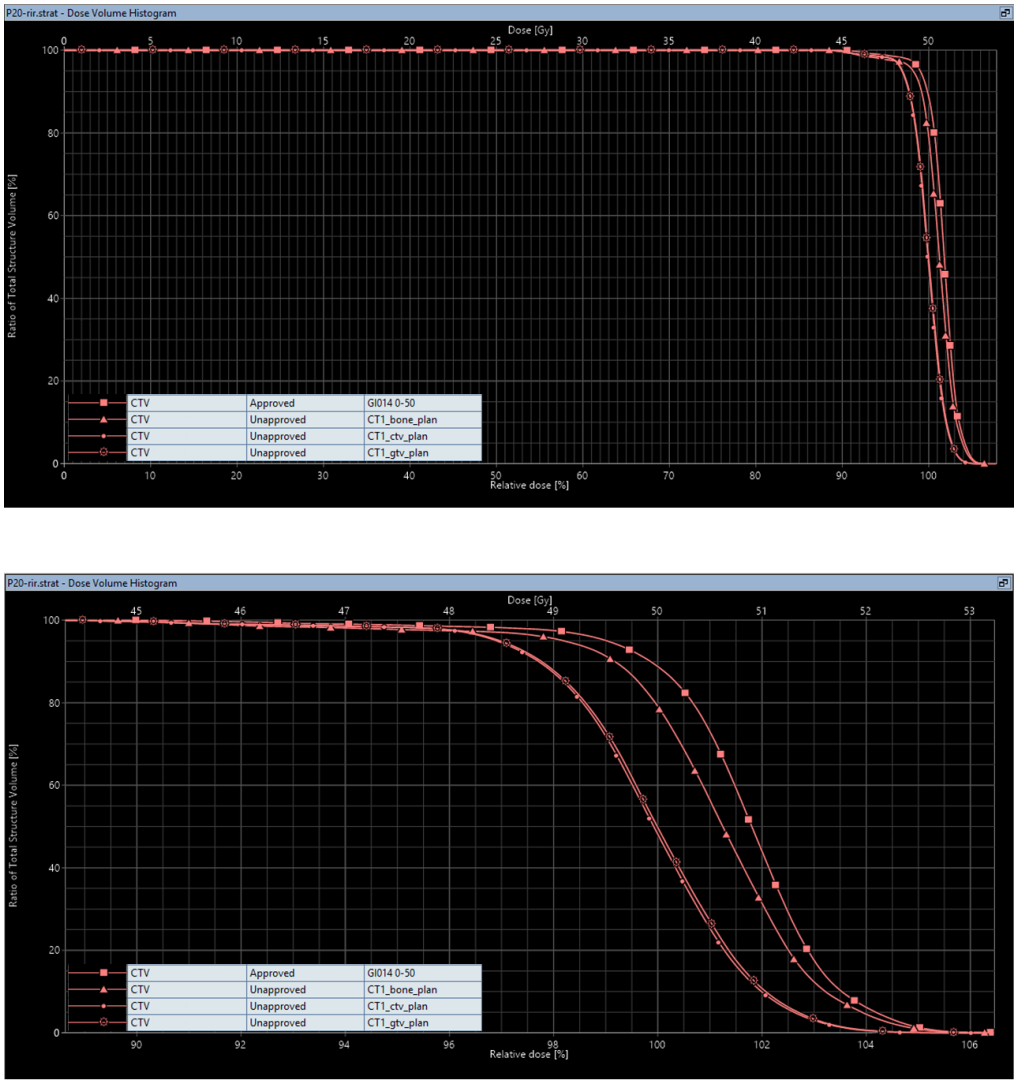

Figure 19: Dose volume histogram showing the effect of different image registration strategies on dose coverage for patient 1 for CTV structure (below image is zoom-in of the above).

- Patient 2:

  This patient had also only primary tumor located in the middle. In this DVH graph the original dose plan ”GI014 0-50” (dot symbol) has an noticeable difference from the rest. GTV and CTV (square & triangle symbols) show similar trend as the previous patient, however the dose distribution that described by the bone match, deviates significantly from the original dose plan. This might happen due to quite curvy spine making the registration procedure challenging leading to a mismatch.

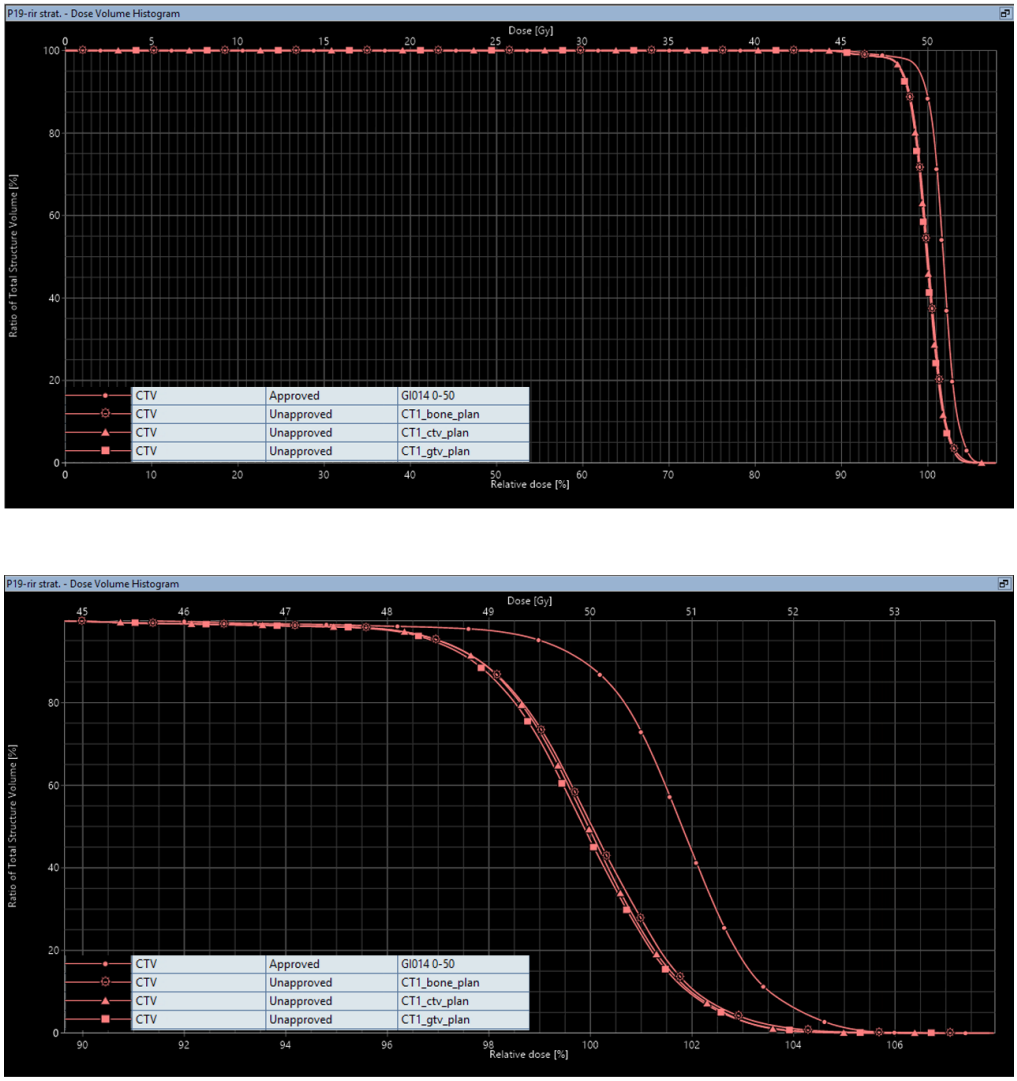

Figure 20: Dose volume histogram showing the effect of different image registration strategies on dose coverage for patient 2 for CTV structure (below image is zoom-in of the above).

- Patient 3: This patient had only primary tumor located in the upper part of the spine. In the current patient all of the tested strategies (triangle symbol-bone strategy,circle symbol-gtv strategy & dot symbol-ctv strategy) appear to have similar DVH curves with each other, and they do not deviate significant with the curve of the original plan ”GI014 0-50” (square symbol).

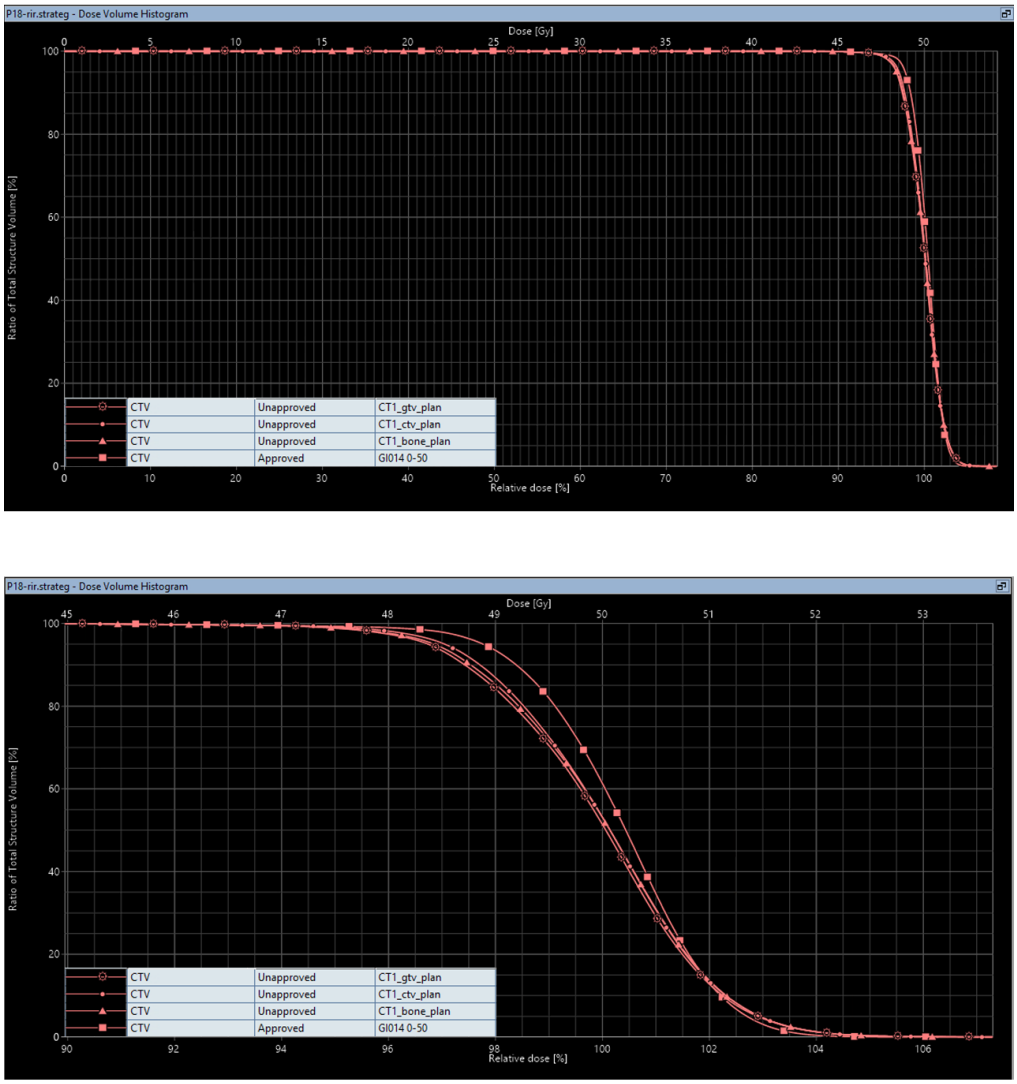

Figure 21: Dose volume histogram showing the effect of different image registration strategies on dose coverage for patient 3 for CTV structure (below image is zoom-in of the above).

5.2 ANATOMICAL CHANGES

As for the anatomical changes, the following DVH graphs for each patient demonstrate the CTV coverage on each CBCT of the adapted CT. Since in the first part of the results we observed that the ”Bone match” was quite better (for patient 1 & 3) than the rest we choose to proceed with this registration strategy for the dose coverage testing. Each CBCT is represented by an individual geometric shape as the attached table in the graph shows in each case.

- Patient 1:

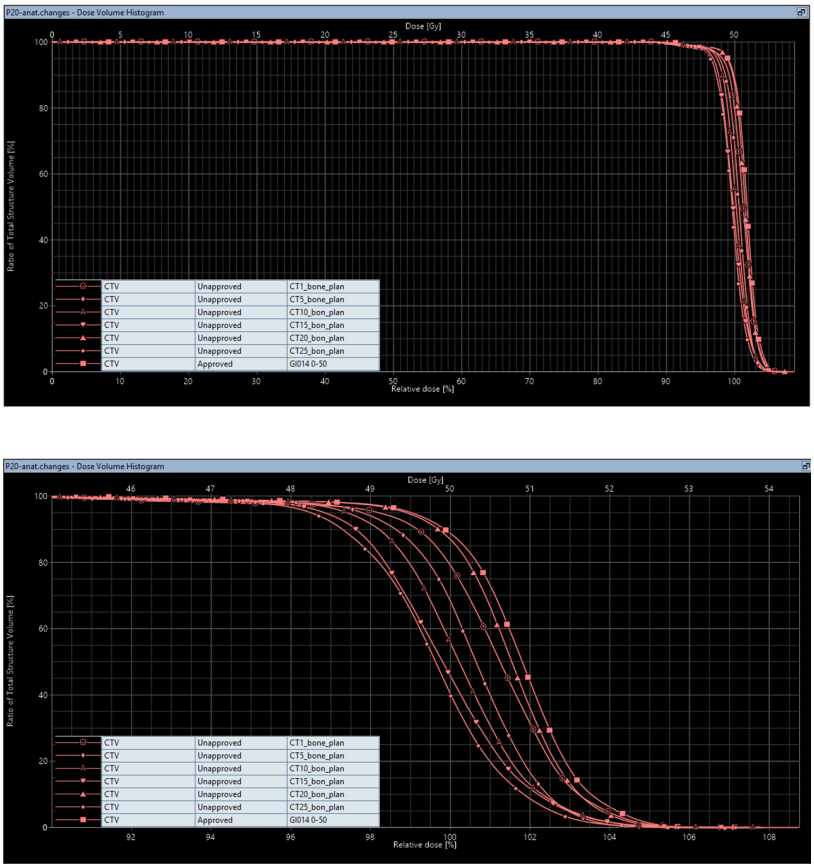

Figure 22: Dose volume histogram showing the effect of anatomical changes on CTV dose coverage for patient 1 (below image is zoom-in of the above).

- Patient 2:

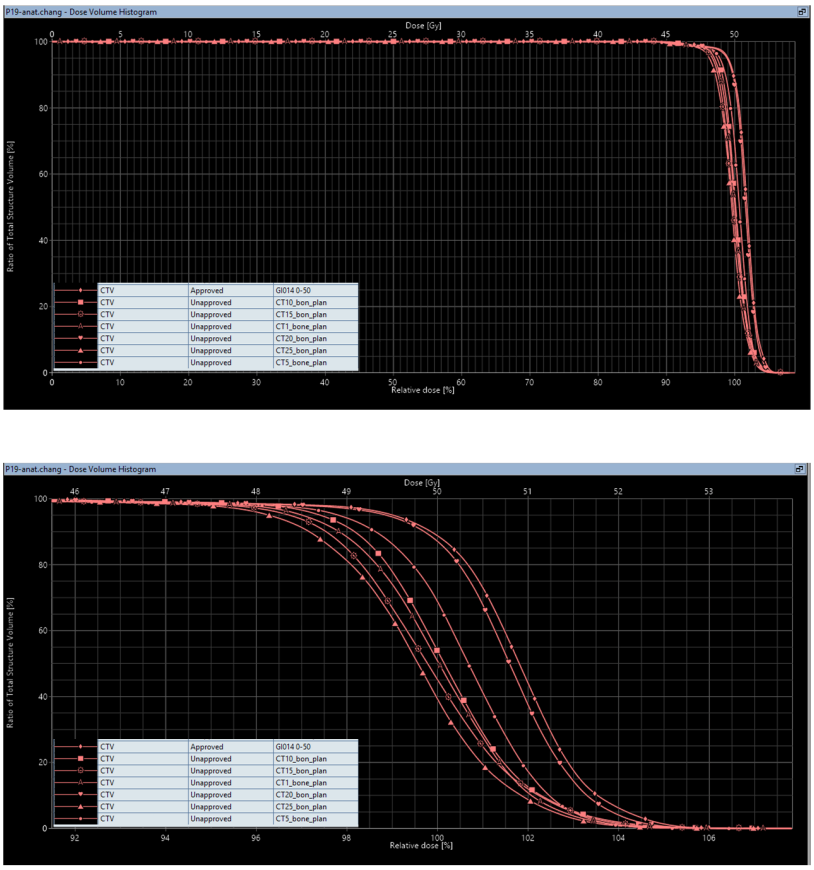

Figure 23: Dose volume histogram showing the effect of anatomical changes on CTV dose coverage for patient 2 (below image is zoom-in of the above).

- Patient 3:

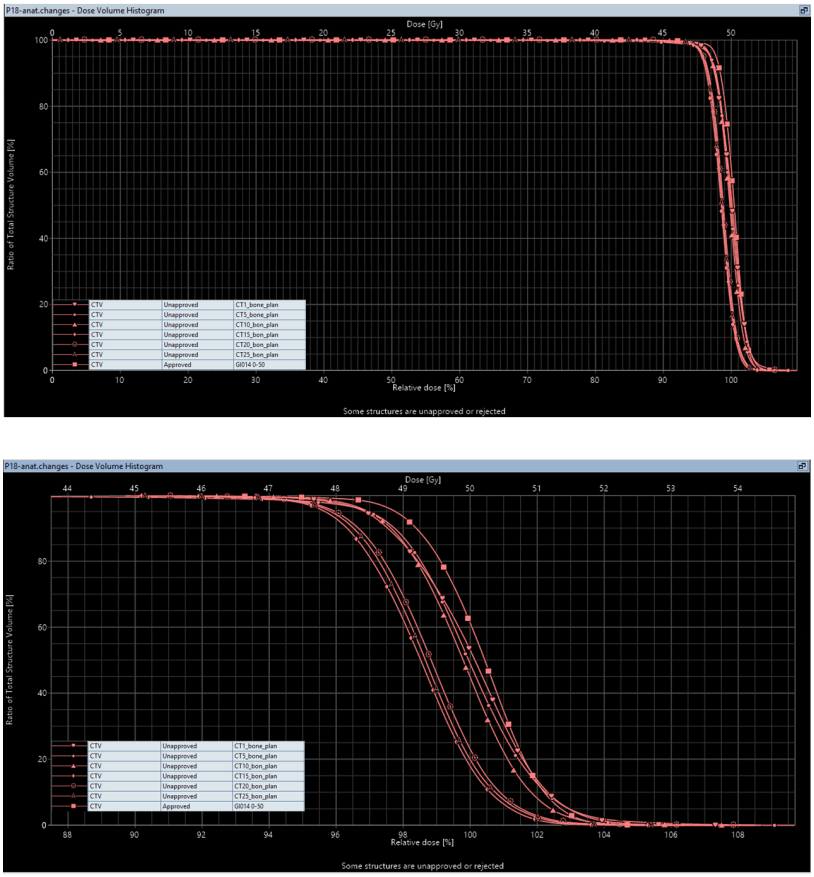

Figure 24: Dose volume histogram showing the effect of anatomical changes on CTV dose coverage for patient 3 (below image is zoom-in of the above).

In all three cases, we observe that each adapted CT dose plan gradually deviates to a significant extent from the original dose plan (”GI014 0-50”). This could indicate a considerable change in the body anatomy resulting an underdose plan and furthermore the need of ongoing dose planning. However, our results are not perfectly ”linear”. In particular, if we take a closer look in the fig. 22 the adapted dose for CT20 (rhombus shape) has a similar curve as the CT1 (square shape) and both are very close to the original dose plan.

Part IV

DISCUSSION AND FUTURE WORK

6

DISCUSSION

This project tested the hypothesis of ”soft tissue” matching as the golden truth, surprisingly turned out that our assumption did not hold as our histograms were not following a normal distribution and our margin values were larger than 7mm, since the margin formula of van Herk excludes rotational errors the organ motion has been underestimated and our margin values considered as a lower limit. A nice confirmation of our results in Part I were the dose volume histograms in Part II which show the dose coverage on CTV as well as the effect of anatomical changes.

6.1 MAIN FINDINGS:

6.1.1 *Part I:*

- The SD of results reproducibility was small, however might be some individual cases where the variation is large as the range values shows.
- All three RIR strategies had lower systematic than random uncertainties, which is preferred since systematic ensures the accuracy of the dose distribution.

- Our hypothesis on ”perfect soft tissue match” did not hold and this was clear from histograms (fig. 15) and the poor correlation between the two soft tissue matches (fig. 17).

- Our PTV margin values for bone match under the assumption of ”perfect soft tissue match” were larger than the clinical limits (7mm). In the case where our assumption was true, then the clinical margins would be too small. However, since our hypothesis does not hold, our margin values cannot considered as valid.

6.1.2 *Part II:*

- The DVH of the adapted (soft tissue match) CTs shows under-dosage effect for the three studied patients. However, there is an indication that bone match adapted CTs is better since it performed similar curve as the original dose.

- The anatomical changes seem to have a dominant influence in dose distribution. During the treatment course, the daily dose curves deviate with each other, this result would indicate the need of a re-adjustment of the dose plan.

7

FUTURE WORK

A bigger dataset would lead us to more reliable and clear conclusions, however, the available time for this project was limited and the study of more patients was not possible. In the results section, we have focused only on the CTV dose coverage which is the clinical target volume and thus the most important target structure. The rest of body structures need to be examined as well as the organs at risk like the heart, spine, lungs, and other. Radiotherapy aims not only to efficient dose coverage but also to eliminate the radiation to surrounding healthy tissue. Complementary to this project, the errors and uncertainties through all the RIR and DIR procedures should be calculated in order to evaluate the reliability of our results. During RIR and DIR there were cases where registrations were challenging to be performed because of patient's very curvy spine or blurry CBCT scans.In that case, a deep test on reproducibility of registrations is essential. The duration of the project allowed to test only a small part of the data, however we would have a better picture of human effect by reproducing the results several times by different researchers.

Part V

APPENDIX

APPENDIX

Below we show the DVH showing the effect of different image registration strategies for the rest 5 adapted CBCTs that we tested on dose coverage for patient 1 (fig. 25a-25e) and 2 (fig. 26a-26e). The figure 27 shows the difference in the matching of the planning CT and a CBCT, more specifically shows patient 1 during the RIR focusing on soft tissue match (CTV) of the CBCT 25.

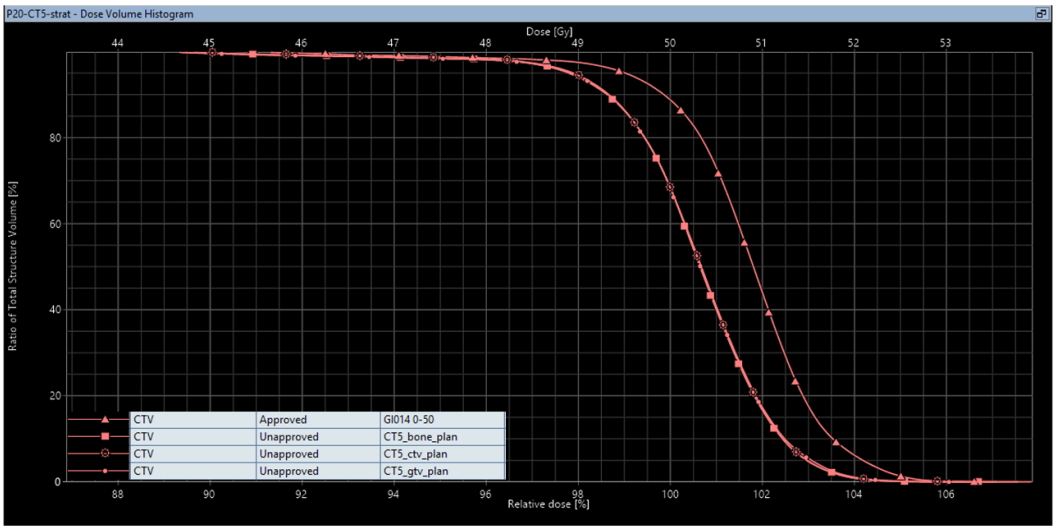

(a) Dose volume histogram showing the effect of different image registration strategies during the fifth day of treatment (CT5) on dose coverage for patient 1 for CTV structure

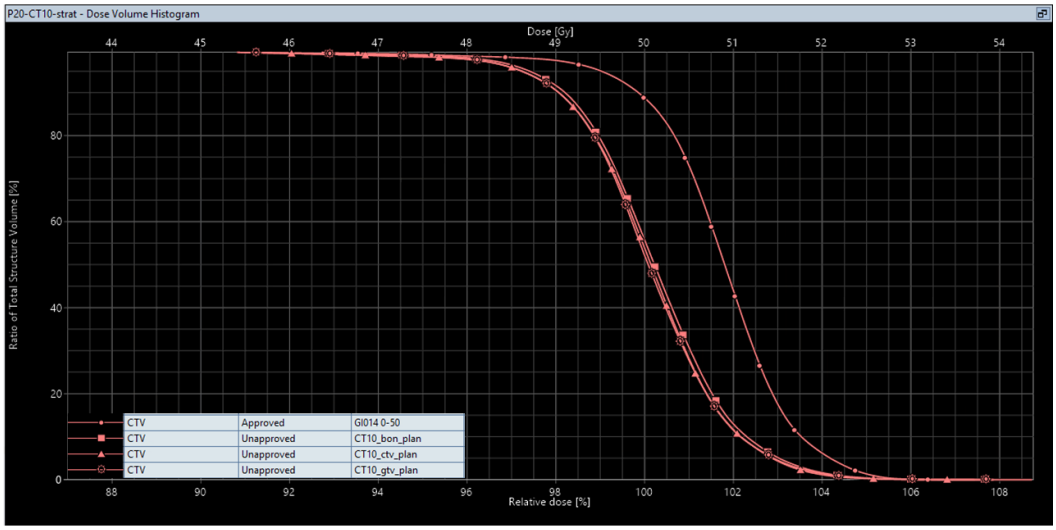

(b) Dose volume histogram showing the effect of different RIR strategies during the tenth day of treatment (CT10) on dose coverage for patient 1 for CTV structure

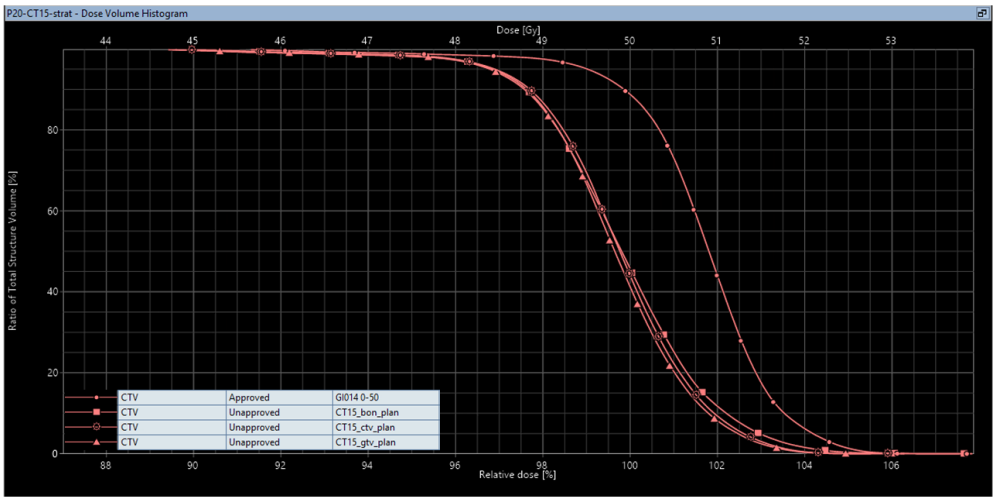

(c) Dose volume histogram showing the effect of different RIR strategies during the 20th day of treatment (CT15) on dose coverage for patient 1 for CTV structure

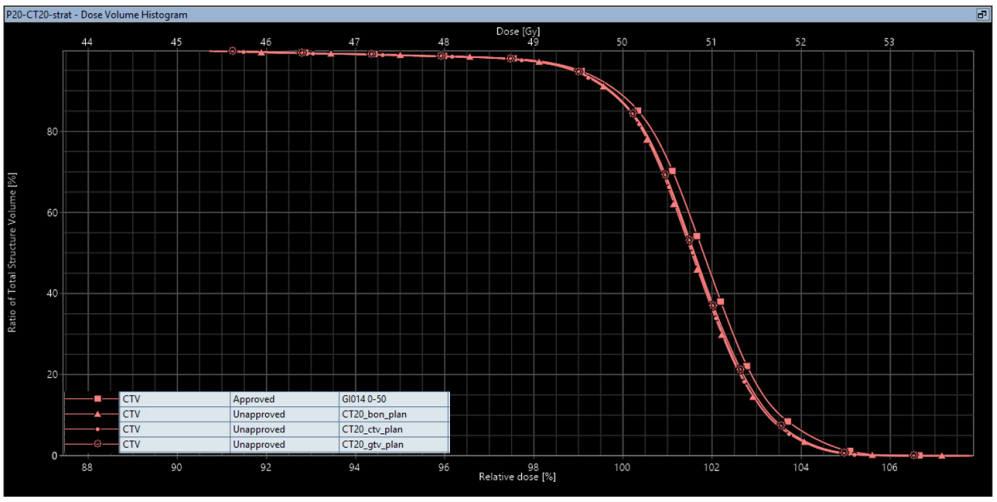

(d) Dose volume histogram showing the effect of different RIR strategies during the 15th day of treatment (CT20) on dose coverage for patient 1 for CTV structure

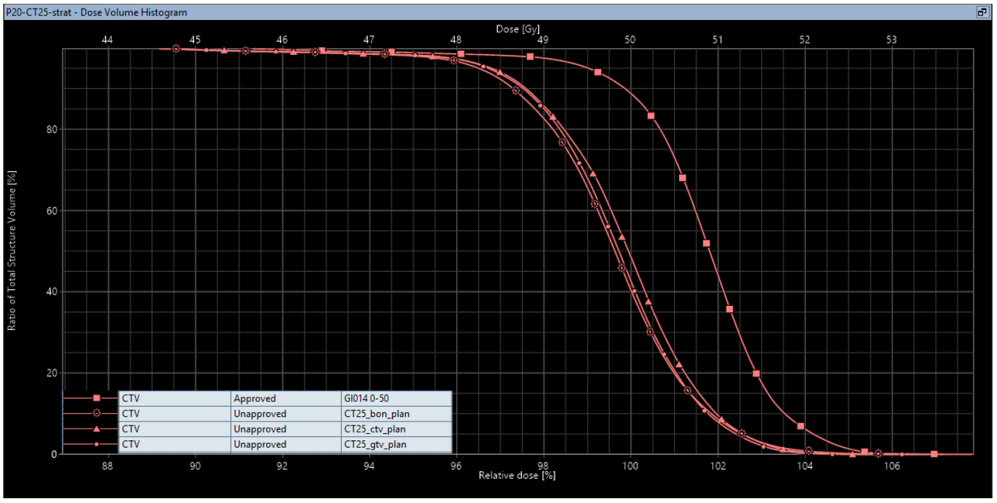

(e) Dose volume histogram showing the effect of different RIR strategies during the 25th day of treatment (CT25) on dose coverage for patient 1 for CTV structure

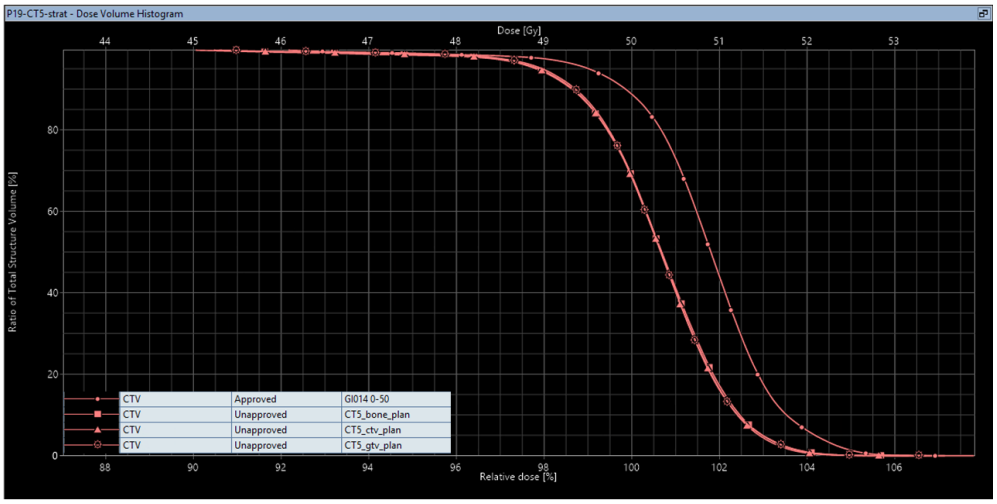

(a) Dose volume histogram showing the effect of different RIR strategies during the fifth day of treatment (CT5) on dose coverage for patient 2 for CTV structure

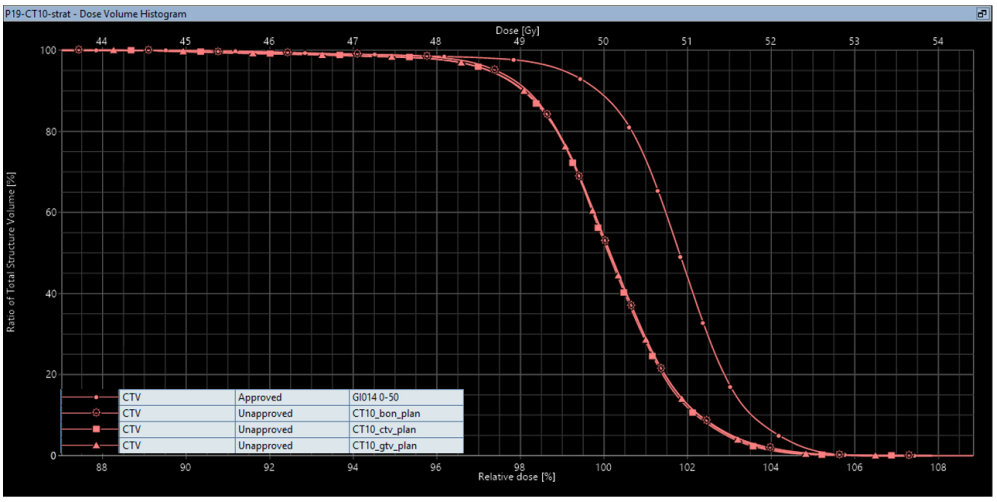

(b) Dose volume histogram showing the effect of different RIR strategies during the tenth day of treatment (CT10) on dose coverage for patient 2 for CTV structure

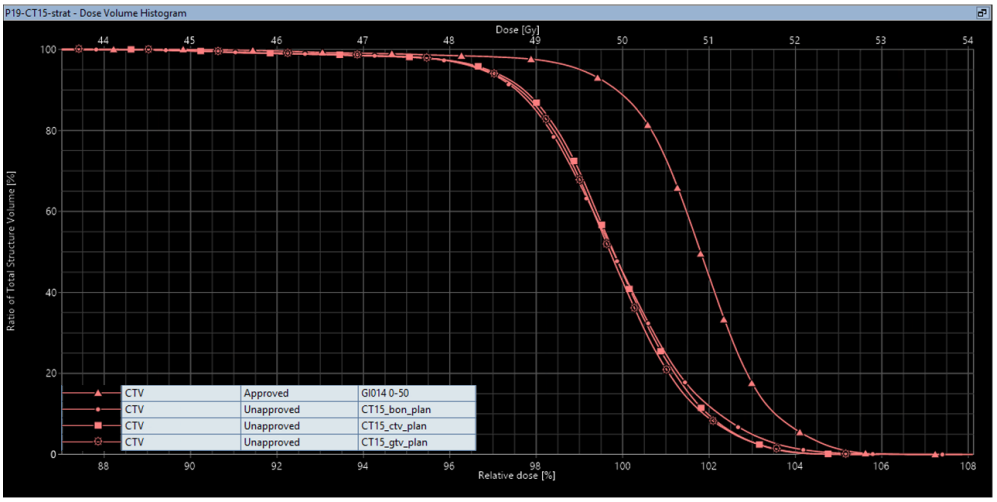

(c) Dose volume histogram showing the effect of different RIR strategies during the 15th day of treatment (CT15) on dose coverage for patient 2 for CTV structure

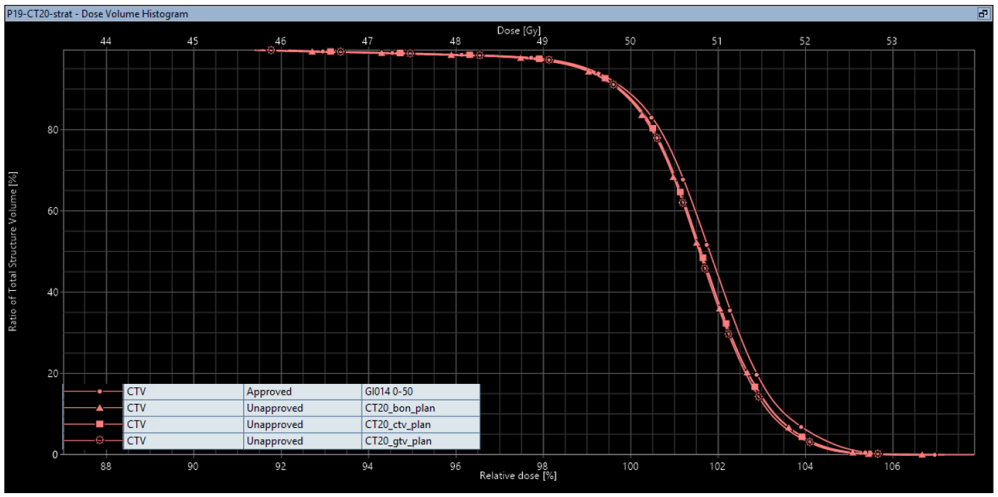

(d) Dose volume histogram showing the effect of different RIR strategies during the 20th day of treatment (CT20) on dose coverage for patient 2 for CTV structure

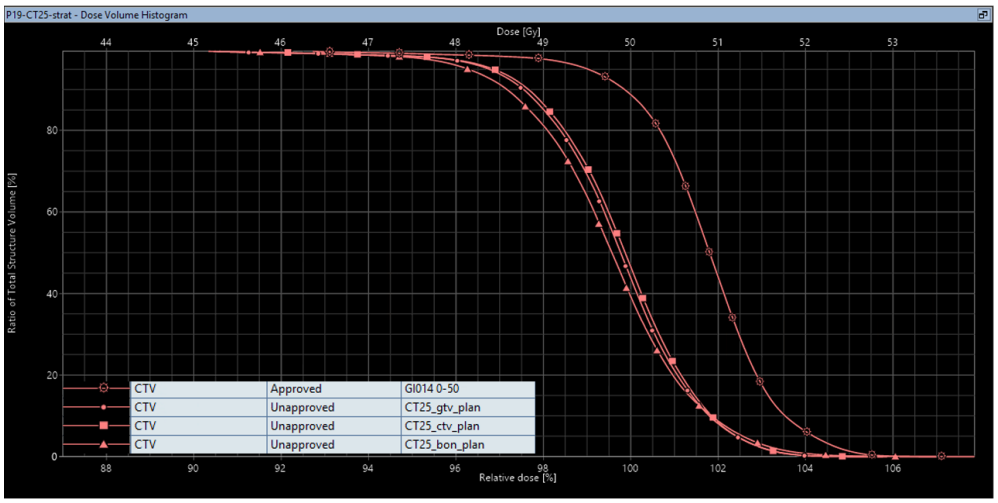

(e) Dose volume histogram showing the effect of different RIR strategies during the 25th day of treatment (CT25) on dose coverage for patient 2 for CTV structure

Figure 26: DVH showing the effect of different RIR strategies during the rest 5 adapted CBCTs for patient 2.

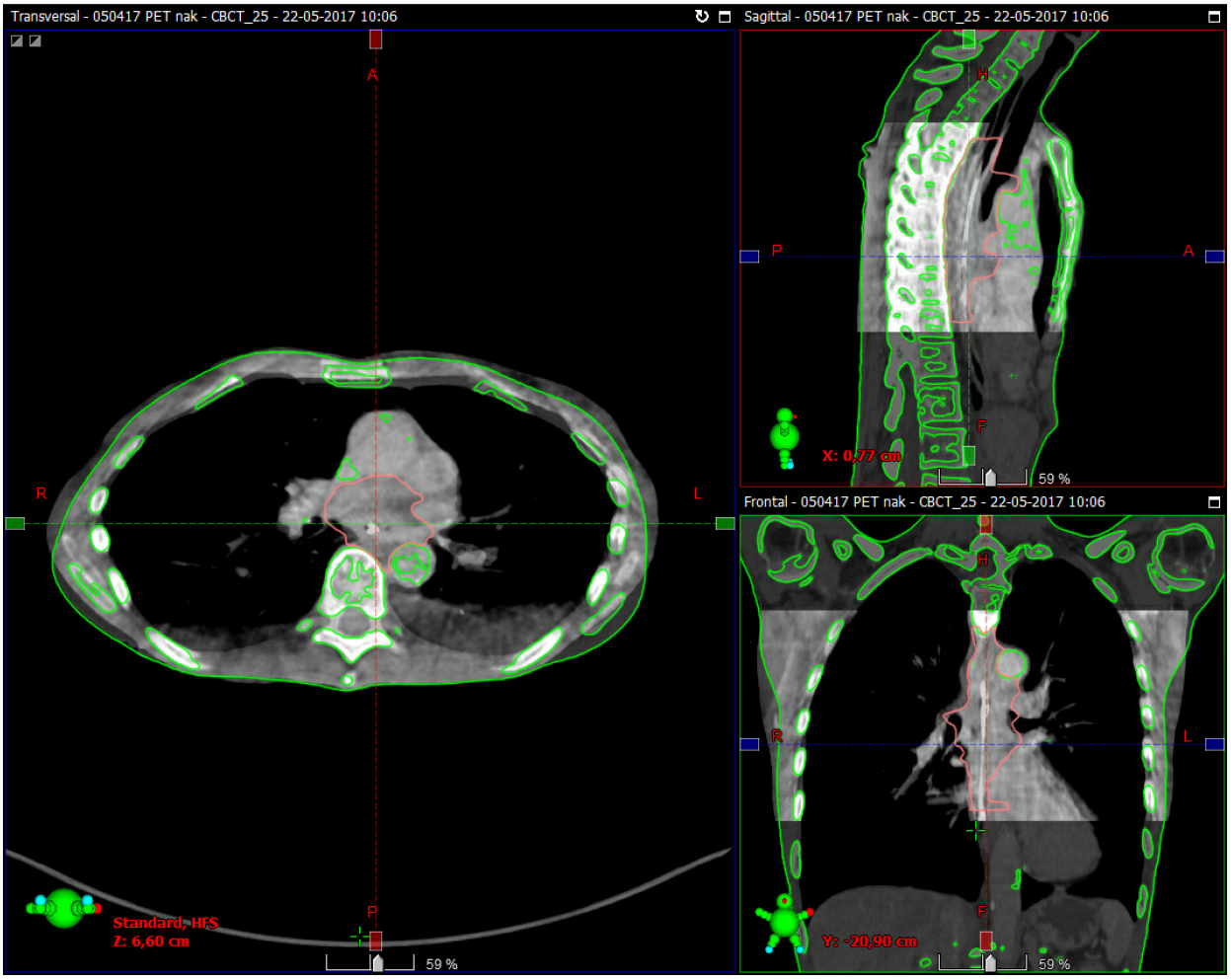

Figure 27: Difference between the planning CT and CBCT25 during soft tissue matching.

Part VI

REFERENCES

BIBLIOGRAPHY

BOOKS

[1] Timmerman, Robert D., and Lei Xing. "Image-guided and adaptive radiation therapy", Lippincott Williams & Wilkins, 2012.

[2] Mayles, Philip, Alan Nahum, and Jean-Claude Rosenwald. "Handbook of radiotherapy physics: theory and practice", CRC Press, 2007.

[3] O'Rahilly, Ronan, and Fabiola Müller. Basic human anatomy: a regional study of human structure. WB Saunders Company, 1983.

PAPERS

[4] International Commission on Radiation Units and Measurements. ICRU Report 83 Prescribing, Recording, and Reporting Photon-beam Intensity-modulated Radiation Therapy (IMRT)-Journal of the ICRU-Vol 10 No 1 2010. Oxford University Press, 2010.

[5] International Commission on Radiation Units and Measurements. ICRU Report 62 Prescribing, Recording and Reporting Photon Beam Therapy (Supplement to ICRU Report 50) (1999).

[6] Van Herk, Marcel, et al. ”The probability of correct target dosage: dose-population histograms for deriving treatment margins in radiotherapy.” International Journal of Radiation Oncology Biology Physics 47.4 (2000): 1121-1135.

[7] Brock, Kristy K., et al. ”Use of image registration and fusion algorithms and techniques in radiotherapy: Report of the AAPM Radiation Therapy Committee Task Group No. 132.” Medical physics 44.7 (2017): e43-e76.

[8] Machiels, Mélanie, et al. ”Comparison of carina-based versus bony anatomy-based registration for setup verification in esophageal cancer radiotherapy.” Radiation Oncology 13.1 (2018): 48.

[9] Fortin, Dominique, et al. ”Deformable versus rigid registration of PET/CT images for radiation treatment planning of head and neck and lung cancer patients: a retrospective dosimetric comparison.” Radiation Oncology 9.1 (2014): 50.

[10] Athanasiou, Lambros S., Dimitrios I. Fotiadis, and Lampros K. Michalis. Atherosclerotic Plaque Characterization Methods Based on Coronary Imaging. Academic Press, 2017.

[11] Oh, Seungjong, and Siyong Kim. ”Deformable image registration in radiation therapy.” Radiation oncology journal 35.2 (2017): 101.

[12] Middleton, Mark, et al. ”Online versus offline corrections: opposition or evolution? A comparison of two electronic portal imaging approaches for locally advanced prostate cancer.” Radiographer 53.1 (2006): 24-28.

WEBSITES

[13] American Cancer Society (n.d.). Esophagus cancer. Retrieved from: https://www.

cancer.org/cancer/esophagus-cancer.html

[14] Cancer Research UK (n.d.). Oesophageal cancer. Retrieved from: https://www.cancerresearchuk.org/about-cancer/oesophageal-cancer/stages-types-and-grades/stage-1